Thoracic adaptations for ventilation during locomotion in humans and other mammals

W. Éamon Callison, Nicholas B. Holowka and Daniel E. Lieberman

Department of Human Evolutionary Biology, Harvard University, 11 Divinity Avenue, Cambridge, MA, USA

ABSTRACT

Bipedal humans, like canids and some other cursorial mammals, are thought to have been selected for endurance running, which requires the ability to sustain aerobic metabolism over long distances by inspiring large volumes of air for prolonged periods of time. Here we test the general hypothesis that humans and other mammals selected for vigorous endurance activities evolved derived thoracic features to increase ventilatory capacity. To do so, we investigate whether humans and dogs rely on thoracic motion to increase tidal volume during running to a greater extent than goats, a species that was not selected for endurance locomotion. We found that while all three species use diaphragmatic breathing to increase tidal volume with increasing oxygen demand, humans also use both dorsoventral and mediolateral expansions of the thorax. Dogs use increased dorsoventral expansion of the thorax, representing an intermediate between humans and goats. 3D analyses of joint morphology of 10 species across four mammalian orders also show that endurance-adapted cursorial species independently evolved more concavo-convex costovertebral joint morphologies that allow for increased rib mobility for thoracic expansion. Evidence for similarly derived concavo-convex costovertebral joints in *Homo erectus* corresponds with other evidence for the evolution of endurance running in the genus *Homo*.

KEY WORDS

Respiration, thorax, human evolution, ribcage, bipedalism, endurance running

INTRODUCTION

Humans differ from other non-human primates, including chimpanzees, in being adapted more for endurance than for power and speed (Carrier, 1984; Bramble and Lieberman, 2004; O'Neill et al., 2017; Pontzer, 2017). Like other primates, chimpanzees rarely sprint and do so only for short distances of less than 100 m, followed by resting and intense panting (Hunt, 1991; Bramble and Lieberman, 2004). In contrast, humans are capable of sustained endurance activities such as trekking and endurance running, defined as running long distances (>5 km) over extended time periods using aerobic metabolism (Bramble and Lieberman, 2004). In humans, endurance running requires breathing as much as 1.3-2.5 $L \cdot min^{-1} \cdot kg^{-1}$ (mass-specific minute ventilation; Weibel, 1984; Bulbulian et al., 1986). Only a few other running-adapted (cursorial) mammals, including dogs, wolves, camels and horses, are known to be capable of such sustained aerobic capacity (Coombs, 1978; Garland, 1983; Carrano, 1999). Among these species' adaptations for endurance running are increased maximal oxygen intake ($\dot{V}O_{2MAX}$) and respiratory capacity (Taylor et al., 1980; Seeherman et al., 1981; Gehr et al., 1981; Hildebrand, 1988; Bramble, 1989; Lindstedt et al., 1991; Poole and Erickson, 2011), and the ability to increase the volume of air inspired per breath (tidal volume; V_T) and per minute (minute ventilation, $\dot{V}_E$; Berry et al., 1996; Poole and Erickson, 2011) while changing the pattern of ventilatory and locomotory coordination (Bramble and Carrier, 1983; Bramble, 1989; Carrier, 1996; Boggs, 2002; Daley et al., 2013).

The human lung can meet the demands of aerobically intense exercise by increasing V_T up to 10-fold (Dempsey, 1985). However, the thoraco-abdominal elongation used by quadrupeds to increase V_T during locomotion (Marlin et al., 2002) may be physically constrained in humans by the arrangement of the viscera and the position of the thoracic cavity above the abdominal viscera due to upright bipedality. It is unknown whether the uniquely shaped human thorax contributes to its respiratory capabilities. Most research concerning the evolution of hominin thoracic morphology has focused on the transition from funnel- to barrel-shaped chests. Reconstructions indicate that fossils of *Australopithecus afarensis* (AL-288-1) and *Au. sediba* (MH1 and MH2) have generally ape-like funnel-shaped thoraxes (although the upper thorax of one partial skeleton of *Au. afarensis*, KSD-VP-1/1, has been argued to be barrel-shaped; Haile-Selassie et al., 2010). In contrast, fossils in the genus *Homo*, including *H. erectus* (KNM-WT15000) and *H. neanderthalensis*, typically have more barrel-shaped or bell-shaped thoraxes (Schmid, 1983; Trinkaus, 1983; Jellema et al., 1993; Franciscus and Churchill, 2002; Sawyer and Maley, 2005; Gómez-Olivencia et al., 2009; Haile-Selassie et al., 2010; Schmid et al., 2013; García-Martínez et al., 2014; Latimer et al., 2016; Bastir et al., 2017), though the preserved elements of *H. naledi* suggest a narrow upper thorax and wide lower thorax (Williams et al., 2017).

Here we test the general hypothesis that humans, like other mammals apparently selected for vigorous endurance activities such as long-distance running, evolved derived thoracic features to increase ventilatory capacity. Normal, quiet inspiration in humans results almost entirely from intrathoracic volume changes caused by the contraction and flattening of the diaphragm (Weibel, 1984). In addition to diaphragmatic contraction, two main integrated types of movement permit the ribs to expand thoracic cavity size: the pump-handle (PH) and bucket-handle (BH) motions (Figure 1). In the PH motion the upper ribs pivot around their vertebral articulations, elevating their anterior ends and the attached sternum, expanding the thorax dorsoventrally. In contrast, the BH motion expands the thorax in the coronal plane by swinging the ribs that are attached to the body of the sternum (in humans, ribs 2-7) laterally and rotating them around both their vertebral and sternal articulations. As the ribs move cranially and caudally with both types of movement, the mediolateral and dorsoventral diameters of the rib cage change. PH and BH motions, and the resulting dorsoventral and mediolateral expansions, have been documented in immobilized, anesthetized dogs and cats during forced ventilation (Da Silva et al., 1977; Margulies et al., 1989), humans (Jordanoglou, 1970; Wilson et al., 1987; Saumarez, 1986), crocodylians (Brocklehurst et al., 2017), and squamates (Brainerd et al., 2016). Changes in thoracic dimensions have also been measured in running horses (Colborne et al., 2006; Thorpe et al., 2009).

Because it is difficult to measure how thorax shape might affect respiration in large numbers of species, we also explore here an alternative source of

information, the morphology of the costovertebral joints. Costovertebral joint morphology has been assumed to reflect rib motion during locomotion in mammals because PH and BH rib movements originate at these joints. Joint surface curvature could provide an indication of overall joint mobility, with more curved joint surfaces theoretically indicating greater ranges of rib motion that might allow for increased dorsoventral and mediolateral thoracic expansion (Hamrick, 1996), but this has never been tested. Here we determine whether concavo-convex joint morphology is present in animals known to increase thoracic volume through dorsoventral and/or mediolateral thoracic expansion and in animals known to engage in endurance behavior. If increased concavo-convex joints are observed, we can make predictions about potential thoracic motion in animals that we have not measured experimentally, including fossil species. Increased joint surface curvature is associated with increased mobility in many joints, but analyses of costovertebral joint structure in iguanas and alligators illustrate the difficulties of reconstructing rib movement based on joint morphology alone (Brainerd et al., 2016; Brocklehurst et al., 2017). In addition, intercostal function changes between ventilation and locomotion in lizards (Carrier, 1991) and birds (Codd et al., 2005; Tickle et al., 2007). Furthermore, variations in intercostal muscle function in dogs suggest that rib motion and thoracic function might change depending on locomotor behavior (Carrier, 1996), and that rib motion is different ipsilateral and contralateral to the forelimb of support during trotting (Bramble and Jenkins, 1993).

Here, to test if costovertebral joint shape in the thorax of humans and other endurance-adapted cursorial species facilitates dorsoventral and mediolateral thoracic expansions that increase ventilatory capacity, we integrate experimental and comparative data to test four hypotheses. First, humans are predicted to supplement diaphragmatic respiration with dorsoventral and mediolateral thoracic expansions to increase overall volumetric expansion of the thoracic cavity during aerobically challenging activities in order to overcome constraints on ventilation due to bipedality. Second, dogs, which are an endurance-adapted cursorial animal, are predicted to supplement diaphragmatic breathing with thoracic movements, but primarily with dorsoventral rather than mediolateral thoracic expansion. Dogs are predicted to rely more on dorsoventral expansion because, like most cursorial quadrupeds, they have deep and narrow rib cages (resulting from flattened ribs with reduced lateral curvature and rib angles) that physically limit mediolateral thoracic expansion (Bramble, 1989). Furthermore, dogs are predicted to rely more on dorsoventral expansion because they must use their forelimbs to support body weight via a thoracic muscular sling that attaches the scapula directly to the thorax (Carrier et al., 2006), meaning mediolateral thoracic expansion could move the forelimbs in a way that might de-stabilize the forelimb joints during locomotion. Third, animals that employ more dorsoventral and/or mediolateral thoracic expansions to augment V_T are hypothesized to have more rounded costovertebral joint facets in which one articular surface is convex while its corresponding surface is concave, allowing for greater rotation around the ribs' long axes and more flexion for increased BH

and PH rib movements (Figure 1). Finally, if this is true, we hypothesize that species known to engage in endurance running will have more curved joint surfaces than those that do not.

MATERIALS AND METHODS

Assessment of Thoracic Function

Subjects

Thoracic movement and respiration were measured in three species: humans, goats and dogs. For humans, ten healthy, male adults with no history of major neuromuscular, cardiovascular or respiratory disease were recruited. Only male participants with BMI <25 were used to facilitate placement of surface markers directly on the skin of the thorax with minimal extraneous skin movement. All participants provided written informed consent, and prior approval for the experiments was obtained from the Committee on the Use of Human Subjects, Harvard University.

To compare humans with quadrupeds, three female Nubian goats (*Capra hiricus*) and three (2 males and 1 female) greyhound dogs (*Canus familiaris*) were also measured. Whereas dogs are endurance-adapted cursorial species, goats do not run long distances, have lower $\dot{V}O_{2MAX}$ relative to body mass than similarly sized cursors (Taylor et al., 1980), and are not considered very cursorial (Carrano, 1999). Harvard University Institutional Animal Care and Use Committee approval was obtained for the study, and institutional animal care guidelines were followed throughout.

Kinematics/Experimental Trials

All running was measured on treadmills. Human participants ran on an instrumented Bertec treadmill (Bertec, Columbus, OH); dogs and goats ran on a custom-built treadmill (Kram, 1989). All subjects wore heart rate (HR) monitors (Polar, New York, NY) placed around the chest cranial to the xiphoid process. To facilitate cross-species comparisons and to measure a range of exercise intensities, human participants completed a series of trials on the treadmill at rest and running at approximately 40%, 60%, 80% and 100% of maximum heart rate (HR_{MAX}). HR_{MAX} in humans was measured by having participants run on a treadmill at increasing speeds and inclines until HR plateaued at maximum effort.

Dogs and goats had $\dot{V}O_2$ and associated HR measured using a Sable Systems Oxygen Analyzer (Sable Systems, NV, PA-10) while trotting at the fastest speeds they would sustain (2.0 to 2.23 $m \cdot s^{-1}$ for goats; 2.8 to 3.0 $m \cdot s^{-1}$ for dogs). Estimated HR_{MAX} values (Table S1) were calculated based on these measurements and previously measured $\dot{V}O_{2MAX}$ values for dogs (Lucas et al., 1980) and for goats (Taylor et al., 1980; $Estimated\ HR_{MAX} = \frac{HR_{measured} \times VO_{2MAX}}{VO_{2measured}}$). Dogs also completed a similar series of trials on the treadmill at rest and while running at heart rates that ranged between 35% and 50% of estimated HR_{MAX}. Goats completed a similar series of trials on the treadmill at rest and while running at heart rates that ranged between 60% and 100% of HR_{MAX}. When measuring thoracic motion, human speeds ranged from 1.3 $m \cdot s^{-1}$ to 5.1 $m \cdot s^{-1}$, goat speeds ranged from 1.5 $m \cdot s^{-1}$to 2.23 $m \cdot s^{-1}$ (trotting), and dog speeds ranged from 1.25 $m \cdot s^{-1}$to 3.0 $m \cdot s^{-1}$ (trotting). Inspiratory flow and volume were

measured using a spirometer (ADInstruments, Colorado Spring, CO, ML311) attached to a one-way flow respirometry mask with outputs recorded using Lab Chart spirometry software (AD Instruments, Colorado Spring, CO). We measured respiration rate (f_R) and V_T at increasing HRs (Table S1).

To record thoracic movements in humans, 26 reflective markers were applied to the thorax (Figure 2). Five markers, evenly spaced between C7 and T12, were used to define the spine. An additional six markers were used to define the dorsal portion of the thorax, arranged in three evenly spaced rows from the thoracic inlet to the lower costal margin. Nine markers were similarly placed on the ventral thorax, with three used to distinguish the sternum, from manubrium to xiphoid process. Three markers were placed under both arms on the lateral aspects of the thorax.

Due to differences in shape and size, the thoraxes of goats and dogs were covered with 16 markers and 18 markers, respectively (Figure 2). In these species, three evenly spaced markers were used to define the spine, and three evenly spaced markers were used to distinguish the sternum from manubrium to xiphoid process. In goats, five markers in two evenly spaced rows placed on both sides defined the lateral aspects of the thorax from the thoracic inlet to the lower costal margin. In dogs, six markers in two rows of three defined the lateral aspects of the thorax. In order to reduce surface marker errors due to extraneous movement of hair and skin, goats had small portions of their thorax shaved to facilitate marker placement. Lean, shorthaired greyhounds were used as canine subjects to reduce possible marker error from hair and skin movement.

Furthermore, markers were placed on thoracic regions lacking substantial subcutaneous soft tissue and away from forelimb musculature.

Marker data were captured at 200 Hz using eight infrared Oqus cameras (Qualisys Corp, Gothenburg, Sweden) positioned around the treadmill. Marker data were cleaned in Qualisys (Qualisys Corp, Gothenburg, Sweden) and processed in a custom-written MATLAB (MathWorks, Natick, MA) program (written by WÉC) to calculate the volume of the thorax with respect to time. The program creates a 3D representation of the thorax in Euclidean space by connecting each point to every other measured point, using a triangular convex hull to generate a 3D shape from these points, and calculates the volume contained within the maximum 3D shape (Orthogonal Fit Ratio=0.999; see Statistical Analysis). Thorax volume was calculated from each frame over the course of ten complete breaths per experimental condition. Maximum dorsoventral thoracic expansion was measured as the maximum change in distance between the most protruding pair of markers on the sternum and spine; maximum dorsoventral thoracic expansion was measured using the most protruding pair of markers on the lateral aspects of the thorax. From these measurements, PH and BH rib motions were inferred.

Statistical Analysis

Data analysis was performed in JMP Pro 13 (SAS Institute Inc., Cary, NC) and R (R Core Team, 2014). Because mammalian lung volume scales isometrically with body mass (Gehr et al., 1981), V_T was standardized by each subject's body mass. Likewise, maximum dorsoventral and mediolateral thoracic

expansions were standardized by subject chest depth and width (average chest depth and width during the trial), respectively. Changes in thoracic volume were measured as the difference in thoracic volume between inspiration and expiration. The change in thoracic volume per breath was then standardized to the average volume of the thorax for each trial and calculated as percent changes to allow cross-species comparisons.

To account for repeated measures and nonparametric data, nonlinear mixed effects models using generalized least squares were used to assess fixed effects on thoracic response variables across species. Individual subject ID was included as a random effect and subjects were treated as a random sample from larger populations. Differences in slope between groups were assessed using a repeated measures ANCOVA. Differences in resting thoracic volume change relative to thoracic volume were assessed using a pairwise Tukey's HSD.

Finally, to assess the reliability and accuracy of our volumetric calculations of thoracic volume, we used the above methods to measure the volume of a standard cylinder of known volume. Our volumetric assessment method was then tested using an orthogonal regression test examining the linear relationship between two continuous variables and comparing expected volume measurements to those observed/measured.

Measurements of Costovertebral Joint Morphology

Measurements were taken from skeletons with complete or near-complete rib cages and vertebral columns from the following species: *Homo sapiens* (N=7; 3 adult males, 1 sub adult male, and 3 adult females), *Pan troglodytes* (N=7; 2 adult males, 2 adult females, 2 adults of unknown sex, and one juvenile of unknown sex), *Capra hiricus* (N=3; adult females), *Canus familiaris* (N=2; adults of unknown sex), *Canus lupus* (N=2; 1 adult female, 1 adult of unknown sex), *Ursus americanus* (N=3; 1 male adult, 1 female adult, and 1 adult of unknown sex), *Equus caballus* (N=3; adults of unknown sex), *Camelus dromedarius* (N=2; 1 male adult and 1 adult of unknown sex), *Rhinoceros unicornis* (N=1; 1 adult of unknown sex), *Dicerorhinus sumatrensis* (N=1; 1 adult of unknown sex), and *Merycoidodon culbertsoni* (N=2; 2 specimens of unknown sex and age). 3D images were also collected from research casts of the four hominin species with well-preserved thoraxes: *Australopithecus afarensis* (AL-288), *Au. sediba* (MH1 and MH2), *H. erectus* (KNM-WT15000) and *H. neanderthalensis* (Shanidar 2, Shanidar 3 and Dederiyeh 2). Modern human, australopith and *H. erectus* specimens were selected from the Peabody Museum of Archaeology and Ethnology, quadrupedal specimens from the Museum of Comparative Zoology at Harvard University, and Neanderthal specimens the National Museum of Natural History in Washington, D.C. Ribs 4 through 7, as well as corresponding vertebrae, were identified on the basis of length, increasing inferior angle, and changes in twist of the superior external border following Dudar (1993) and based on notations made during specimen collection and preparation.

The superior and inferior articular facets of ribs 4 through 7, the inferior and transverse costal facets on thoracic vertebra 3, and the superior, inferior and transverse costal facets on thoracic vertebrae 4 through 7 were measured. For each joint, a minimum of 40 photographic images of the ribs' superior and inferior articular facets, as well as a minimum of 60 images of the corresponding superior and inferior costal facets on the corresponding vertebrae, were taken using a Casio EX-XZR100 (Resolution: 4000 x 3000 pixels). Images for each joint were compiled using a photometry program (PhotoScan, Agisoft, St. Petersburg, Russia) to build 3D *in silico* models of the skeletal elements. The models were composed of fine meshgrids containing a minimum of 200,000 faces. The meshgrid faces corresponding to each portion of the costovertebral joint were manually selected to define the contours of the entire joint surfaces in the cranial-caudal plane, and the curvature of each articular facet was then measured using Geomajic software (Geomajic Control, 3D Systems, Rock Hill, SC) by fitting a cylinder to the selected region. For each costovertebral joint facet, Geomajic was also used to measure the radius of curvature as the radius of a cylinder of best fit applied to the entire joint surface, and to calculate the included angle using the measured radius of curvature and measured length of the secant produced at the points where the cylinder of best fit and surface first come into contact. Convex facets were denoted as positive, while concave facets were denoted as negative. Increasing angle value indicates increasing concavo-convexity of the facet. Facets with no curvature in the cranial-caudal plane were designated to have an included angle of 0. The included angle measurement was repeated 5 times for

each element to assess repeatability, and the average was used for data analysis. To test for reliability and accuracy, this method was performed on a cylindrical object of known curvature (Orthogonal Fit Ratio=0.999).

Statistical Analysis

Statistical analysis was performed in JMP Pro 13. To account for repeated measures, a generalized linear mixed model was used to assess the effect of genus and facet type (fixed effects) on costovertebral joint concavo-convexity, as well as the similarity between vertebral and corresponding rib joint facets. Repeated included angle measurements were included as a random effect and specimens treated as a random sample from larger populations. Comparisons for species pairs were assessed with a Tukey's HSD. Cohen's d effect size was used to determine significant differences in included angle of costovertebral joint elements. Following Barrentine (1991), a gauge repeatability test was used to assess the repeatability of individual measurements, with less than 10% measurement variation being rated as "excellent" (Table S2). Despite the potential for error due to the circular nature of angular measurements, we found that linear methods were appropriate to analyze the joint facet data due to the nature of our data (Fig. S1).

RESULTS

Assessment of Ventilation and Thoracic Function

Dorsoventral and mediolateral thoracic expansions differed between all three species (humans, goats and dogs). Maximum dorsoventral expansion increased with mass-specific tidal volume (V_T [L•kg^{-1}]) strongly in humans (m=2.17, SE=0.19, 95% CI [1.80, 2.54], R^2=0.71) and relatively moderately in dogs (m=0.87, SE=0.12, 95% CI [0.63, 1.11], R^2=0.79) at different rates ($p<0.0001$; Figure 3). In contrast, maximum dorsoventral expansion decreased with increasing V_T [L•kg^{-1}] in goats (m=-0.78, SE=0.01, 95% CI [-1.64, 0.07], R^2=0.24), differing significantly from humans ($p<0.0001$) and from dogs ($p=0.0004$). Maximum mediolateral expansion increased with V_T [L•kg^{-1}] in humans (m=1.30, SE=0.12, 95% CI [1.07, 1.53], R^2=0.69; Figure 3). Maximum mediolateral expansion decreased slightly in dogs with V_T [L•kg^{-1}] (m=-0.07, SE=0.32, 95% CI [-0.71, 0.56], R^2=0.0; $p=0.0001$). Maximum mediolateral expansion also decreased in goats with V_T [L•kg^{-1}] (m=-0.77, SE=0.62, 95% CI [-1.98, 0.45], R^2=0.13), differing significantly from humans ($p=0.0016$), but not dogs ($p=0.3255$; Figure 3). Comparisons of maximum dorsoventral thoracic expansion relative to chest depth at maximum V_T [L•kg^{-1}] demonstrate significant differences between dogs and humans (mean=0.079, SE=0.007, 95% CI [0.063, 0.094]) and goats (mean=0.001, SE=0.015, 95% CI [-0.031, 0.033]; $p=0.0003$), and between humans (mean=0.091, SE=0.006, 95% CI [0.078, 0.104]) and dogs and goats (mean=0.020, SE=0.008, 95% CI [0.003, 0.036]; $p<0.0001$). Additionally, maximum mediolateral thoracic expansion relative to chest width at

maximum V_T differed significantly between humans and dogs (mean=0.051, SE=0.004, 95% CI [0.043, 0.060]) and goats (mean=0.002, SE=0.008, 95% CI [-0.016, 0.020]; p=0.0001), and between humans (mean=0.056, SE=0.005, 95% CI [0.046, 0.067) and dogs and goats (mean=0.018, SE=0.006, 95% CI [0.005, 0.032]; p=0.0003).

The change in thoracic volume per breath relative to thoracic volume increased with V_T [L•kg^{-1}] in humans (m=1.72, SE=0.30, 95% CI [1.12, 2.31], R^2=0.37) and weakly but significantly in dogs (m=0.29, SE=0.49, 95% CI [-0.66, 1.24], R^2=0.03; p=0.0146; Figure 4). Conversely, change in thoracic volume decreased with increasing V_T [L•kg^{-1}] in goats (m=-1.30, SE=0.61, 95% CI [-2.50, -0.11], R^2=0.53), unlike humans (p<0.0001) and dogs (p=0.0445; Figure 4). A small difference was observed in resting thoracic volume change relative to thoracic volume between humans (mean=0.041; SE=0.006; 95% CI [0.026, 0.006]) and dogs (mean=0.057; SE=0.010; 95% CI [0.016, 0.100]; p=0.3498), while larger differences were observed between goats (mean=0.004; SE=0.002; 95% CI [-0.006, 0.014]) and humans (p=0.0247) and between goats and dogs (p=0.0085). Overall, humans and dogs have larger thoracic expansions and contractions relative to thoracic volume when at rest than goats and change in thoracic volume during ventilation increases in both dogs and humans, especially, during exercise (Figure 4).

Costovertebral Joint Morphology in Non-Hominids

Within each order examined, cursorial species identified as endurance-adapted have more concavo-convex costovertebral joint elements than related species identified as non-endurance and non-cursorial, which have flatter joints (Figure 5, Fig. S2). Within carnivores, canines have joint elements that are approximately 3- to 10-times more concavo-convex than bears. Within perissodactyls, horses have joint elements that are approximately 2- to 15-times more concavo-convex than rhinoceroses. Finally, within artiodactyls, camels have joint elements that are approximately 2- to 14-times more concavo-convex than goats (and at least 4 times more concavo-convex than *Merycoidodon culbertsoni*, an extinct short-limbed, non-cursorial camel relative; Fig. S3, Table S3).

Significant differences in included angle of the joint elements between species identified as endurance-adapted cursors, non-endurance cursors and non-cursors within the same order were observed (Table 1, Table S3). We found that the curvatures of the rib portions of joints are strongly correlated to those of the vertebrae in the lower ($p<0.0001$, $R^2=0.77$) and upper ($p<0.0001$, $R^2=0.66$) portions of the joint in endurance-adapted cursorial species (Figure 5). In non-endurance and non-cursorial species, the curvatures of the rib portions of the joint are weakly correlated to those of the vertebrae in the upper portion of the joint ($p<0.0001$, $R^2=0.31$), but not in the lower portion of the joint ($R^2=0.0$; Figure 5).

Costovertebral Joint Morphology in Hominids

H. sapiens have joint elements that are 11- to 51-times more concavo-convex than *P. troglodytes* ($p<0.0001$; Figure 5 and 6; Fig. S2; Tables 1 and 2). *Au. afarensis* joint facets are not significantly different than chimpanzees (superior costal facet, $p=1.00$; inferior costal facet, $p=0.9986$), nor are those of *Au. sediba* (superior costal facet, $p=0.9999$; inferior costal facet, $p=0.9726$; superior articular facet, $p=0.9932$; inferior articular facet, $p=1.00$; Table 2, Figure 6). *H. sapiens* costovertebral joint elements are considerably more concavo-convex than those of *Au. afarensis* (superior costal facet, $p=0.0001$; inferior costal facet, $p=0.0033$), and 12- to 69-times more concavo-convex than *Au. sediba* (superior costal facet, $p<0.0001$; inferior costal facet, $p<0.0001$; superior articular facet, $p=0.0094$; inferior articular facet, $p=0.0087$; Table 2, Figure 6).

H. erectus has the same distinctive configuration as *H. sapiens*, with convex vertebral facets (superior costal facet, $p=0.9274$; inferior costal facet, $p=0.9996$) and concave rib facets (inferior articular facet, $p=0.9995$; Figure 6). *H. erectus* has joint elements that are more concavo-convex than *Au. afarensis* (superior costal facet, $p=0.0048$; inferior costal facet, $p=0.0077$), approximately 15- to 72-times more concavo-convex than *Au. sediba* (superior costal facet, $p=0.0002$; inferior costal facet, $p<0.0001$; inferior articular facet, $p=0.1788$), and approximately 12- to 46-times more concavo-convex than chimpanzees (superior costal facet, $p<0.0001$; inferior costal facet, $p<0.0001$; inferior articular facet, $p=0.0700$; Table 2, Figure 6).

Finally, *H. neanderthalensis* specimens exhibit a costovertebral joint morphology similar to other species of the genus *Homo*. Like *H. sapiens*, *H. neanderthalensis* has convex vertebral facets (superior costal facet, p=0.3986; inferior costal facet, p=0.2957) and concave rib facets (inferior articular facet, p=0.7616; superior articular facet, p=0.3329). *H. neanderthalensis* joint elements are more concavo-convex than *Au. afarensis* (superior costal facet, p=0.0064; inferior costal facet, p=0.1094), approximately 4- to 49-times more concavo-convex than *Au. sediba* (superior costal facet, p=0.0002; inferior costal facet, p=0.0020; inferior articular facet, p=0.3586; superior articular facet, p=0.6509), and approximately 7- to 41-times more concavo-convex than chimpanzees (superior costal facet, p<0.0001; inferior costal facet, p=0.0012; inferior articular facet, p=0.1459; superior articular facet, p=0.3028; Table 2, Figure 6).

DISCUSSION

Aerobically demanding and sustained activities such as long-distance running require increased air intake. First, we experimentally tested whether two species that independently evolved adaptations for endurance cursoriality (humans and dogs) augment diaphragmatic contributions to inspiration by increasing thoracic ventilation relative to V_T during locomotion in comparison to a non-endurance species (goats). To make this comparison, we measured total thoracic volume change with increasing HR and changing V_T. We found that humans had the ability to increase the amount of overall thoracic expansion and contraction per breath as V_T increased (Figure 4) through increased dorsoventral and mediolateral expansions (Figure 3). Dogs maintained almost the same

amount of overall volumetric expansion and contraction of the thorax as V_T increased (Figure 4), but they increased dorsoventral expansion to increase V_T (Figure 3). Goats, however, had limited thoracic expansion during respiration (Figure 3), with less thoracic expansion and contraction per breath as V_T increased (Figure 4).

We also observed that human and dog thoraxes functioned differently as predicted in terms of mediolateral expansion. As V_T increased, humans increased both the amount of dorsoventral and mediolateral thoracic expansion per breath. In contrast, dogs only increased dorsoventral expansion, and to a lesser extent than humans. Dogs also slightly decreased mediolateral expansion as they increased V_T, accounting for the differences in overall thoracic expansion observed between humans and dogs. The observed lack of increased mediolateral expansion per breath with larger V_T suggests that mediolateral thoracic expansion generated by BH rib motion is limited in dogs, who represent and intermediate between humans and goats.

This limitation may extend to other cursorial quadrupeds for several reasons. First, endurance-adapted cursors, like dogs and horses, have greater $\dot{V}O_{2MAX}$'s than expected for their body masses (Poole and Erickson, 2011). This ability to effectively and efficiently transport oxygen into the body, along with the ability to increase the volume of the thorax via thoraco-abdominal elongation during trotting and galloping (Marlin et al., 2002), may have reduced selection for increased thoracic expansion during ventilation while aerobically active. Simply put, quadrupedal endurance-adapted cursors like dogs may not need to rely on

mediolateral thoracic expansion to increase the volume of the thorax. The observed increase in dorsoventral expansion, and the resulting change in overall thoracic volume, may suffice.

Second, cursorial quadrupeds need to support their body weight with their forelimbs by keeping each forelimb in a parasagittal plane. As described in horses (McGuigan and Wilson, 2003; Beck and Clayton, 2013) and dogs (Carrier et al., 2006), the trunk of cursorial quadrupeds is suspended between the forelimbs by a muscular thoracic sling (Kardong, 1998). Portions of this thoracic sling, including the m. *serratus ventralis*, directly connect the cervical transverse processes and sternal ribs to the dorsomedial aspect of the scapula and control the position of the scapulae relative to the thorax (Davis, 1949; Gray, 1968; Beck and Clayton, 2013). BH motion of the sternal ribs and the resulting mediolateral thoracic expansion would therefore cause mediolateral motion of the scapula during locomotion because the scapula attaches directly to the dorso-lateral surface of the rib cage. Decreased movement in the parasagittal plane might increase the stability of the shoulder during locomotion and might be resisted by force imposed by the limb.

Finally, another likely explanation of reduced mediolateral thoracic expansion in dogs is the typical shape of the quadrupedal cursor thorax. Most cursorial mammals have evolved deep and narrow rib cages with shortened costal cartilages and ribs that are highly flattened mediolaterally (Hildebrand, 1988; Bramble, 1989), thereby reducing the lateral curvature of the chest and resulting in limited mediolateral expansion when the ribs swing upwards in the

BH motion. This characteristic chest shape may have been selected for to reduce bending moments on the ribs during locomotion (Bramble, 1989). Thus, selection to reduce loading the thorax has resulted in a rib shape that also limits BH motion, and therefore mediolateral thoracic expansion. However, the thoracic structure typical of quadrupedal cursors is not observed in bipedal cursors, such as humans and kangaroos (Bramble, 1989) who have more laterally curved chests, so when the ribs swing upwards in these species a larger change in the lateral dimension of the thorax. Thus, more BH motion and mediolateral thoracic expansion occur.

Unlike in quadrupedal cursors who rely on thoraco-abdominal elongation to increase V_T during galloping and trotting (Marlin et al., 2002), thoraco-abdominal elongation during locomotion may be constrained in humans, who walk and run bipedally with the thoracic cavity positioned above the abdominal viscera. Because humans do not rely on a thoracic sling to support the forelimbs and because the human thorax does not follow the typical cursorial thoracic bauplan, bipedalism allows for increased mediolateral and dorsoventral thoracic expansion of the thorax. Thus, to compensate for restrictions on increasing thoracic volume cranial-caudally due to bipedality, we hypothesize that humans instead rely on both greater dorsoventral expansion as well as mediolateral expansion to increase the volume of the thorax during aerobic ventilation. However, as in quadrupeds, increased rib mobility and thoracic movement likely involves a tradeoff between stability and increased ventilatory ability. The configuration of the upper thorax and scapula in chimpanzees has been argued

to be associated with arboreal locomotion in order to resist large bending moments generated by contractions of the thoracoscapular muscles (Hunt, 1991; Preuschoft, 2004). Furthermore, trunk stability and increased stiffness for proximal muscle attachments may improve muscle force production in the extremities needed for quick and powerful movements (Hodges et al., 1997; Jensen et al., 2000). Increased rib mobility might require increased respiratory muscle activation and increasing intrathoracic pressure to stabilize the rib cage during arboreal locomotion and might reduce the ribs' abilities to resist bending moments during arm loading. Thus, thoracic mobility and thoracic expansion may have been constrained in hominins such as australopiths that continued to rely on arboreal climbing.

Based on our data, if the modern human thorax were as constrained in terms of expansion as a goat's, a 71 kg (average body mass of this study's participants) human's maximum V_T would be approximately 2.25 L, around 47% of typical human vital capacity and approximately 79% of the average maximum V_T (2.84 L) measured in our human participants. In addition, maximum $\dot{V}_E$ [$L \cdot min^{-1} \cdot kg^{-1}$] would be reduced to 1.97 $L \cdot min^{-1} \cdot kg^{-1}$ (based on an observed maximum respiration rate of 62 breaths per minute), an approximate 9% reduction in the maximum measured $\dot{V}_E$ [$L \cdot min^{-1} \cdot kg^{-1}$].

Our experimental results predict greater costovertebral concavo-convexity in humans and dogs than in goats. As expected, we found that humans and dogs have 2-10 times more concavo-convex costovertebral joint elements than goats. Based on this finding, endurance-adapted cursorial species should have more

concavo-convex articular facets on the ribs and bodies of the vertebrae than closely related non-endurance and non-cursorial species. Increased joint concavo-convexity should permit greater rotation around the ribs' long axes and more flexion for increased dorsoventral and mediolateral thoracic expansions due to more BH and PH motion, respectively. We found that endurance-adapted cursorial species have 2-51 times more concavo-convex costovertebral joint elements than non-endurance and non-cursorial species from the same order, which have flatter joints (Figure 5, Fig. S2). In particular, humans have joint elements that are more concavo-convex than chimpanzees, canids have joint elements that are more concavo-convex than bears, horses have joint elements that more concavo-convex than rhinoceroses, and camels have joint elements that are more concavo-convex than goats (and more concavo-convex than a non-cursorial ancestor, *Merycoidodon*; Fig. S3, Table S3). Given that mammals, unlike reptiles, ventilate while they locomote and endurance-adapted cursorial species have more concavo-convex costovertebral joint elements (from which rib movements originate), increased joint concavo-convexity likely indicates the ability for the thorax to undergo larger expansions and contractions during each breath using either dorsoventral expansion alone or in conjunction with mediolateral expansion.

Based on the measured differences in joint morphology across taxa, it appears that the costovertebral joint has been subject to convergent selective pressures across several orders to facilitate increased sustained aerobic capacity. The observation that increased costovertebral concavo-convexity is

present to some extent in all the endurance-adapted cursorial species surveyed and is lacking in non-endurance and non-cursorial species suggests that increased joint curvature helps facilitate large V_T that, along with changes f_R, are necessary for long-distance running. Furthermore, comparisons of extant camels and *Merycoidodon* (an extinct short-limbed, non-cursorial terrestrial herbivore and camel ancestor; Clifford, 2010) suggest that increased concavo-convexity was selected for following the evolution of endurance cursoriality in camelids (Fig. S3). As one might predict from convergent evolution, the pattern of increased concavo-convexity differs in some of these cursorial species. Camels have increased the curvature of the upper portion of the costovertebral joint relative to goats and *Merycoidodon*, with an almost ball-and-socket configuration. Furthermore, whereas the rib facets of the joint are convex and the vertebral facets are concave in endurance-adapted cursorial carnivores, artiodactyls and perissodactyls, this pattern is reversed in humans, whose rib facets are concave and vertebral facets are convex (Figure 5, Fig. S2). We infer that humans independently evolved a novel costovertebral joint architecture to facilitate increased thoracic expansion and contraction, hence V_T, during sustained long-distance bipedal running. As with many other skeletal adaptations for running, this shift appears to coincide with the origins of the genus *Homo* (Bramble and Lieberman, 2004). Together, these morphological data and kinematic experiments support the hypothesis that humans, like dogs and other endurance-adapted cursorial species, independently experienced selection to increase thoracic volumetric change during aerobic respiration by increasing the concavo-

convexity of the costovertebral joints, which, in turn, permit greater dorsoventral and mediolateral thoracic expansions (from increased PH and BH motions, respectively) to increase V_T as needed.

This study has several limitations. First, the costovertebral joint can be subject to damage and deterioration in fossil samples, making measurements approximate. We found the heads of ribs in Neanderthal specimens to be especially damaged. Second, our study only compares thoracic ventilation between three species, only two quadrupedal species were studied experimentally, and sample sizes were small due to the limited number of available subjects. Future studies should include a wider variety of cursorial and non-cursorial species and more subjects. Furthermore, limitations on subject training constrained the speeds at which we could safely run the dogs and goats. As such, thoracic ventilation in goats and dogs was only measured while the animals rested, walked and trotted. Thus, our results do not reflect how the thorax might function during galloping in quadrupeds, which may be different due to dissimilarities in entrainment and respiratory mechanics between gaits (Bramble and Carrier, 1983; Bramble, 1989; Boggs, 2002). However, cursorial quadrupeds use thoraco-abdominal elongation to expand the thoracic cavity and increase V_T, with both thoraco-abdominal elongation (Marlin et al., 2002) and V_T (Szlyk et al., 1981) increasing most during galloping. This increase in thoracic volume, coupled with highly efficient cardiovascular and muscular systems and high $\dot{V}O_2$ (Poole and Erickson, 2011), makes it unlikely that cursorial animals would increase thoracic ventilation only during trotting when not used during

galloping, though this is a topic for future research. Third, our goat subjects may have been stressed when measured at rest, resulting in possibly inflated measurements of resting V_T or f_R relative to previous studies (Smith et al., 1983). However, because the purpose of this study was to measure the relationship between thoracic ventilation and V_T, our goats taking possibly larger or faster breaths at rest would not affect our conclusions. Fourth, the use of surface markers can lead to error in kinematic measurements due to the motion of skin and underlying subcutaneous fat. Future experiments using X-ray Reconstruction of Moving Morphology (XROMM) would provide more accuracy and precision. We are nonetheless confident in our results because we used multiple markers to measure change in thoracic volume during expansion and contraction across multiple breaths and because we attempted to limit the amount of extraneous marker motion (Figure 2). Fifth, costovertebral joint movement itself was not measured, but rather inferred from overall thoracic expansion and contraction. XROMM experiments could shed light on how the joint itself moves during locomotion. Finally, chest shape and size varies among humans, and the human participants in this study were selected from college-age males living at sea level. Thus, another avenue for future research is to test if there are any differences in thoracic expansion patterns between males and females and among populations with long-term exposure to high elevation.

Although more research is needed to test the relationship between costovertebral morphology and thoracic movement during high intensity aerobic activity, the above results in combination with morphological measurements on costovertebral joints in the hominin fossil record allow us to speculate about selection for enhanced ventilatory capacity in human evolution. While thoracic size influences overall respiratory volume, our results suggest that rib mobility is also a key feature of aerobic respiration. As noted above, modern humans have a unique costovertebral joint morphology in which the rib facets of the costovertebral joint are convex and the vertebral facets are concave (Figure 5, Fig. S2). This unique joint morphology appears to be evident in all species of the genus *Homo* (though there is increased variation in the articular facets of *H. neanderthalensis*, likely due to wear and damage common in fossil ribs) but is lacking in australopiths and great apes (Figure 6). Because lung volume scales isometrically with body mass in mammals (interspecific slope=1.06; Gehr et al., 1981), we can approximate thoracic volume changes in hominin species based on estimated body mass and assuming modern human-like dorsoventral and mediolateral thoracic expansions from costovertebral joint shape. Using an estimated body mass of 51.4 kg (Grabowski et al., 2015) and assuming similar thoracic motion to modern humans, we estimate that *H. erectus* would have had a thoracic volume change during inspiration and expiration at HR_{MAX} approximately 0.27 L greater than a similar-sized chimpanzee, resulting in an additional oxygen intake of 16.73 $L \cdot min^{-1}$ from increased thoracic ventilation alone. Although $\dot{V}O_{2MAX}$ is affected by muscle fiber composition (Bergh et al.,

1978), mitochondrial density and other variables affected by aerobic training (Astrand and Rodahl, 1986), we can nonetheless approximate the effect of increased thoracic motion on *H. erectus* $\dot{V}O_{2MAX}$. By calculating expected $\dot{V}O_{2MAX}$ from body mass (Calder, 1981) for an average chimpanzee male ($\dot{V}O_{2MAX}$=2.2 L•min^{-1}, M_B=39 kg), calculating expected $\dot{V}O_{2MAX}$ for a 71 kg modern human male ($\dot{V}O_{2MAX}$=3.564 L•min^{-1}), and comparing these values to the measured average $\dot{V}O_{2MAX}$ in modern human males ($\dot{V}O_{2MAX}$=4.5 L•min^{-1}; Bergh et al., 1978), we estimate that *H. erectus* had a $\dot{V}O_{2MAX}$ of approximately 3.8 L•min^{-1}, around 38% greater than expected $\dot{V}O_{2MAX}$ calculated from body mass alone. We therefore conclude that the derived human-like costovertebral joint morphology evolved in response to increased selection for high aerobic capacity activities such as endurance running in *Homo* approximately 2 million years ago.

LIST OF SYMBOLS AND ABBREVIATIONS

BH	bucket-handle
C7	7th cervical vertebra
f_R	respiration rate (breaths/min)
HR	heart rate
HR_{MAX}	maximum heart rate
IAF	inferior articular facet
ICF	inferior costal facet
M_B	body mass (kg)
PH	pump-handle
SAF	superior articular facet
SCF	superior costal facet
T12	12th thoracic vertebra
V_T	tidal volume (L)
$\dot{V}O_{2MAX}$	maximum amount of oxygen that an individual can utilize during maximal exercise ($LO_2 \bullet min^{-1}$)
$\dot{V}_E$ [$L \bullet min^{-1} \bullet kg^{-1}$]	mass-specific minute ventilation [$L \bullet min^{-1} \bullet kg^{-1}$]
V_T [$L \bullet kg^{-1}$]	mass-specific tidal volume
XROMM	X-ray Reconstruction of Moving Morphology

AKNOWLEDGMENTS

We thank the Harvard Museum of Comparative Zoology, the Peabody Museum of Archaeology and Ethnology and the National Museum of Natural History for access to collections. Statistical support was provided by data science specialist Steven Worthington at the Institute for Quantitative Social Science, Harvard University. We also thank the members of the Skeletal Biology and Biomechanics Lab, especially Ian Wallace and Heidi Nocka, for helping with data collection. We thank the five anonymous reviewers who provided comments that greatly improved the quality of the manuscript. Finally, a special thank you to the humans, animals, and dog-owners that participated in these experiments.

COMPETING INTERESTS

We have no competing interests.

AUTHORS' CONTRIBUTIONS

W.É.C. and D.E.L. designed the experiments. W.É.C. and N.B.H. performed the experiments. W.É.C., N.B.H. and D.E.L. discussed the results, analyzed the data and wrote the manuscript.

FUNDING

This research received no specific grant from any funding agency in the public, commercial or not-for-profit sectors.

DATA AVAILABILITY STATEMENT

Data is available via Dyrad (https://doi.org/10.5061/dryad.9zw3r2299).

REFERENCES

Aiello, L. and Dean, C. (1990). *An Introduction to Human Evolutionary Anatomy*. New York: Academic Press.

Astrand, P. and Rodahl, K. (1986). *Textbook of Work Physiology*. New York, McGraw-Hill.

Barrentine, L.B. (1991). *Concepts for R&R Studies*. Milwaukee, WI: ASQ Quality Press.

Bastir, M., García-Martínez, D., Williams, S.A., Recheis, W., Torres-Sánchez, I., García Río, F., Oishi, M., Ogihara, N. (2017). 3D geometric morphometrics of thorax variation and allometry in Hominoidea. *Journal of Human Evolution* **113**, 10-23. (https://doi.org/10.1016/j.jhevol.2017.08.002)

Beck, W. and Clayton, H. (2013). *Equine Locomotion, 2nd Edition.* Philadelphia: Saunders.

Bergh, U., Thorstensson, A., Sjodin, B., Hulten, B., Piehl, K., Karlsson, J. (1978). Maximal oxygen uptake and muscle fiber types in trained and untrained humans. *Medicine and Science in Sports* **10(3)**, 151-154.

Berry, M.J., Dunn, C.J., Pittman, C.L., Kerr, W.C., Adair, N.E. (1996). Increased ventilation in runners during running as compared to walking at similar metabolic rates. *European Journal of Applied Physiology and Occupational Physiology* **73(3-4)**,245-250. (doi: 10.1007/BF02425483)

Boggs, D.F. (2002). Interactions between locomotion and ventilation in tetrapods. *Comparative Biochemistry and Physiology* A **133**, 269-288.

Brainerd, E., Mortiz, S., Ritter, D. (2016). XROMM analysis of rib kinematics during lung ventilation in the green iguana, *Iguana iguana. Journal of Experimental Biology* **219**, 404-411. (doi: 10.1242/jeb.127928)

Bramble, D.M. (1989). Axial-appendicular dynamics and integration of breathing and gait in animals. *American Zoologist* **29**, 171-186.

Bramble, D.M. and Carrier, D. (1983). Running and breathing in mammals. *Science* **219(4582)**, 251-256.

Bramble, D.M. and Jenkins, F.A. (1993). Mammalian locomotor-respiratory integration: implications for diaphragmatic and pulmonary design. *Science* **262(5131)**, 235-240.

Bramble, D.M. and Lieberman, D.E. (2004). Endurance running and the evolution of Homo. *Nature* **432**, 345–352. (doi: 10.1038/nature03052)

Brocklehurst, R.J., Moritz, S., Codd, J., Sellers, W.I., Brainerd, E. (2017). Rib kinematics during lung ventilation in the American alligator (Alligator mississippiensis): an XROMM analysis. *Journal of Experimental Biology* **220**, 3181-3190. (doi: 10.1242/jeb.156166)

Bulbulian, R., Wilcox, A., Darabos, B. (1986). Anaerobic contribution to distance running performance of trained cross-country athletes. *Medicine and Science in Sport and Exercise* **18(1)**, 107-113.

Calder, W. (1981). Scaling of physiological processes in homeothermic animals. *Annual Review of Physiology* **43**, 301-322. (doi: 10.1146/annurev.ph.43.030181.001505)

Carrano, M.T. (1999). What, if anything, is a cursor? Categories versus continua for determining locomotor habit in mammals and dinosaurs. *Journal of Zoology, London* **247**, 29-42. (doi: 10.1111/j.1469-7998.1999.tb00190.x)

Carrier, D. (1984). The energetic paradox of human running and hominid evolution. *Current Anthropology* **25,** 483-495.

Carrier, D. (1991). Conflict in the hypaxial musculo-skeletal system: documenting an evolutionary constraint. *American Zoologist* **31**: 644-654.

Carrier, D. (1996). Function of the intercostal muscles in trotting dogs: ventilation or locomotion? *Journal of Experimental Biology* **199**, 1455-1465.

Carrier, D., Deban, S., Fischbein, T. (2006). Locomotor function of the pectoral girdle 'muscular sling' in trotting dogs. *Journal of Experimental Biology* **209**: 2224-2237. (doi: 10.1242/jeb.02236)

Clifford, A.B. (2010) The evolution of the unguligrade manus in artiodactyls. *Journal of Vertebrate Paleontology* **30(6)**, 1827-1839. (doi: 10.1080/02724634.2010.521216)

Codd, J.R., Boggs, D.F., Perry, S.F., Carrier, D.R. (2005). Activity of three muscles associated with the uncinate processes of the giant Canada goose *Branta canadensis maximus. Journal of Experimental Biology* **208**, 849-857. (doi: 10.1242/jeb.01489)

Cohen, J. (1988). *Statistical Power Analysis for the Behavioral Sciences*. New Jersey: Routledge.

Colborne, R., Allen, R.J., Wilson, R.J., Marlin, D.J., Franklin, S.H. (2006). Thoracic geometry changes during equine locomotion. *Equine and Comparative Exercise Physiology* **3**, 53-59. (doi: 10.1079/ECP200686)

Coombs, W.P. (1978). Theoretical aspects of cursorial adaptations in dinosaurs. *Quarterly Review of Biology* **53**, 398-418.

Da Silva, K.M., Sayers, B.M., Sears, T.A., Stagg, D.T. (1977). The changes in configuration of the rib cage and abdomen during breathing in the anaesthetized cat. *Journal of Physiology, London* **266**, 499-521.

Daley, M.A., Bramble, D.M., Carrier, D. (2013). Impact loading and locomotor-respiratory coordination significantly influence breathing dynamics in running humans. *PLOS One* **8(8)**, e70752.

Davis, D. (1949). The shoulder architecture of bears and other carnivores. *Fieldiana (Zoolology)* **31**, 285 -305.

Dempsey, J.A. (1985). Is the lung built for exercise? *Medicine and Science in Sports and Exercise* **18**, 143–155.

Dudar, J.C. (1993). Identification of rib number and assessment of intercostal variation at the sternal rib end. *Journal of Forensic Sciences* **38**, 788-797.

Franciscus, R.G. and Churchill, S.E. (2002). The costal skeleton of Shanidar 3 and a reappraisal of Neandertal thoracic morphology. *Journal of Human Evolution* **42**, 303-356.

García-Martínez, D., Barash, A., Recheis, W., Utrilla, C., Torres Sánchez, I., García Río, F., Bastir, M. (2014). On the chest size of Kebara 2. *Journal of Human Evolution* **70**, 69-72.

Garland, T. (1983). The relation between maximal running speed and body-mass in terrestrial mammals. *Journal of Zoology* **199**, 157–170. (doi: 10.1111/j.1469-7998.1983.tb02087.x)

Gehr, P., Mwangi, D.K., Ammann, A., Maloiy, G.M., Taylor, R., Wibel, E.R. (1981). Design of the mammalian respiratory system. V. Scaling morphometric pulmonary diffusing capacity to body mass: wild and domestic mammals. *Respiratory Physiology* **44**, 61-86. (doi: 10.1016/0034-5687(81)90077-3)

Gómez-Olivencia, A., Eaves-Johnson, K.L., Franciscus, R.G., Carretero,, J.M, Arsuaga, J. (2009). Kebara 2: new insights regarding the most complete Neandertal thorax. *Journal of Human Evolution* **57**, 75-90.

Grabowski, M., Hatala, K.G., Jungers, W.L., Richmond, B.G. (2015). Body mass estimates of hominin fossils and the evolution of human body size. *Journal of Human Evolution* **85**, 75-93. (doi: 10.1016/j.jhevol.2015.05.005)

Gray, J. (1968). *Animal Locomotion*. London: Weidenfeld and Nicolson.

Haile-Selassie, Y., Latimer, B.M., Alene, M., Deino, A.L., Gibert, L., Melillo, S.M., Saylor, B.Z., Scott, G.R., Lovejoy, O. (2010). An early *Australopithecus afarensis* postcranium from Woranso-Mille, Ethiopia. *Proceedings of National Academy of Sciences* **107**(27), 12121–12126. (doi: 10.1073/pnas.1004527107)

Hamrick, M.W. (1996). Articular size and curvature as determinants of carpal joint mobility and stability in strepsirrhine primates. *Journal of Morphology* **230**: 113-127. (doi: 10.1002/(SICI)1097-4687(199611)230:2<113::AID-JMOR1>3.0.CO;2-I)

Hildebrand, M. (1988). *Analysis of Vertebrate Structure, 4th Edition*. New York: Wiley & Sons.

Hodges, P.W., Butler, J.E., McKenzie, D.K., Gandevia, S.C. (1997). Contraction of the human diaphragm during rapid postural adjustments. *Journal of Physiology* **505 (Pt 2)**, 539-548.

Hunt, K. (1991). Mechanical implications of chimpanzee positional behavior. *American Journal of Physical Anthropology* **86**, 521-536. (doi: 10.1002/ajpa.1330860408)

Jellema, L.M., Latimer, B., Walker, A. (1993). The rib cage. *The Nariokotome Homo erectus Skeleton*. (Walker, A. and Leakey, R. Eds.). Cambridge: Harvard University Press, 294-325.

Jensen, B.R., Laursen, B., Sjogaard, G. (2000). Aspects of shoulder function in relation to exposure demands and fatigue. *Clinical Biomechanics* **15**, S17–S20.

Jordanoglou, J. (1970). Vector analysis of rib movement. *Respiration Physiology* **10**, 109-120. (doi: 10.1016/0034-5687(70)90031-9)

Kardong, K.V. (1998). *Vertebrates - Comparative Anatomy, Function, Evolution*. Boston: McGraw-Hill.

Kram, R. (1989). A treadmill mounted force platform. *Journal of Biomechanics* **22** (10), 1041. (doi: 10.1152/jappl.1989.67.4.1692)

Latimer, B., Lovejoy, C.O., Haile-Selassie, Y. (2016). The thoracic cage of KSD-VP-1/1. *The postcranial anatomy of Australopithecus afarensis: New Insights KSD-VP-1/1Y*. (Haile-Selassie, Y., Su, D.F. Eds.). Dordrecht : Springer.

Lindstedt, S.L., Hokanson, J.F., Wells, D.J., Swain, S.D., Hoppeler, H., Navarro, V. (1991). Running energetics in the pronghorn antelope. *Nature* **353,** 748-750. (https://doi-org.ezp-prod1.hul.harvard.edu/10.1038/353748a0)

Lucas A., Therminarias, A., Tanche, M. (1980). Maximum oxygen consumption in dogs during muscular excercise and cold exposure. *Pflügers Archiv European Journal of Physiology* **388**, 83-87.

Margulies, S., Rodarte, J., Hoffman, E. (1989). Geometry and kinematics of dog ribs. *Journal of Applied Physiology* **67(2)**, 707-712. (doi: 10.1152/jappl.1989.67.2.707)

Marlin, D., Schroter, R., Cashman, P., Deaton, C., Poole, D., Kindig, C., Mcdonough, P., Erickson, H. (2002). Movements of thoracic and abdominal compartments during ventilation at rest and on exercise. *Equine Veterinary Journal Supplement* **34**, 384-390.

McGuigan, M.P. and Wilson, A.M. (2003). The effect of gait and digital flexor muscle activation on limb compliance in the forelimb of the horse *Equus caballus*. *Journal of Experimental Biology* **206,** 1325-1336. (doi: 10.1242/jeb.00254)

O'Neill, M., Umberger, B., Holowka, N., Larson, S., Reiser, P. (2017). Chimpanzee super strength and human skeletal muscle evolution. *Proceedings of National Academy of Sciences* **114**(28), 7343–7348. (doi: 10.1073/pnas.1619071114)

Pontzer, H. (2017). Economy and endurance in human evolution. *Current Biology*, **27**, R613-R621. (doi: https://doi.org/10.1016/j.cub.2017.05.031)

Poole, D. and Erickson, H. (2011). Highly Athletic Terrestrial Animals: Horses and Dogs. *Comprehensive Physiology* **1**, 1-37.

Preuschoft, H. (2004). Mechanisms for the acquisition of habitual bipedality: Are there biomechanical reasons for the acquisition of upright bipedal posture? *Journal of Anatomy* **204**, 363-384. (doi: 10.1111/j.0021-8782.2004.00303.x)

R Core Team. (2014). R: A language and environment for statistical computing. R Foundation for Statistical Computing, Vienna, Austria. URL http://www.R-project.org/.

Saumarez, R. (1986). An analysis of possible movements of the human upper rib cage. *Journal of Applied Physiology* **60**, 678-689. (doi: 10.1152/jappl.1986.60.2.678)

Sawilowsky, S. (2009). New effect size rules of thumb. *Journal of Modern Applied Statistical Methods* **8** (2), 467–474. (doi: 10.22237/jmasm/1257035100)

Sawyer, G.J. and Maley, B. (2005). Neandertal reconstructed. *Anatomical Record* **283B**, 23-31.

Schmid, P. (1983). A reconstruction of the skeleton of A.L. 288-1 (Hadar) and its consequences. *Folia Primatologia* **40**, 283-306.

Schmid, P., Churchill, S.E., Nalla, S., Weissen, E., Carlson, K.J., de Ruiter, D.J., Berger, L.R. (2013). Mosaic Morphology in the Thorax of *Australopithecus sediba*. *Science* **340**(6129), 109-236. (doi: 10.1159/000156111)

Seeherman, H.J., Taylor, C.R., Maloiy, G.M.O., Armstrong, R.B. (1981). Design of the mammalian respiratory system. II. Measuring maximum aerobic capacity. *Respiratory Physiology* **44**: 11-23.

Smith, C.A., Mitchell, G.S., Jameson, L.C., Musch, T.I., Dempsey, J.A. (1983). Ventilatory Response of Goats to Treadmill Exercise: Grade Effects. *Respiration Physiology* **54**, 331-341.

Szlyk, P.C., McDonald, B.W., Pendergast, D.R., Krasney, J.A. (1981). Control of ventilation during graded exercise in dogs. *Respiration Physiology* **46**, 345-365. (https://doi.org/10.1016/0034-5687(81)90131-6)

Taylor, R., Maloiy, G.M., Weibel, E.R., Langman, V.A., Kanmau, J.M., Seeherman, H.J., Heglund, N.C. (1980). Design of the mammalian respiratory system III. scaling maximum aerobic capacity to body mass in wild and domestic animals. *Respiration Physiology* **44**, 25-37. (doi: 10.1016/0034-5687(81)90075-X)

Thorpe, C.T., Marlin, D.J., Franklin, S.H., Colborne, G.R. (2009). Transverse and dorso-ventral changes in thoracic dimension during equine locomotion. *Veterinary Journal* **179**, 370-377. (doi: 10.1016/j.tvjl.2007.10.014)

Tickle, P.G., Ennos, A.R. Lennox, L.E., Perry, S.F., Codd, J.R. (2007). Functional significance of the unicinate process in birds. *Journal of Experimental Biology* **210**, 3955-3961. (doi: 10.1242/jeb.008953)

Trinkaus, E. (1983). *The Shanidar Neanderthals*. New York: Academic Press.

Weibel, E.R. (1984). *The Pathway for Oxygen*. Cambridge, MA: Harvard University Press.

Williams, S.A., García-Martínez, D., Bastir, M., Meyer, M.R., Nalla, S., Hawks, J., Schmid, P., Churchill, S.E., Berger, L.R. (2017). The vertebrae and ribs of *Homo naledi*. *Journal of Human Evolution* **104**, 136-154. (doi: 10.1016/j.jhevol.2016.04.008)

Wilson, T.A., Rehder, K., Krayer, S., Hoffman, E.A., Whitney, C.G., Rodarte, J.R. (1987). Geometry and respiratory displacement of human ribs. *Journal of Applied Physiology* **62**, 1872-1877. (doi: 10.1152/jappl.1987.62.5.1872)

Figures

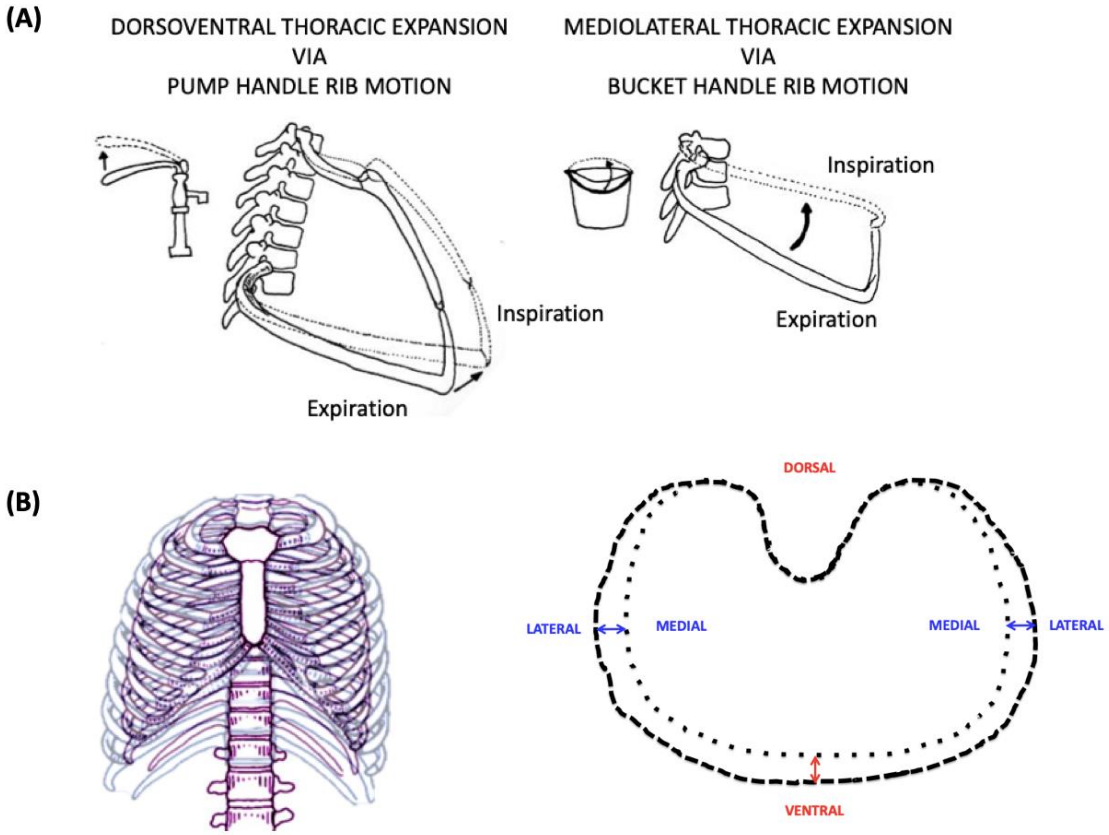

Figure 1: (A) The pump-handle and bucket-handle rib movements that expand the thorax dorsoventrally and mediolaterally, respectively. Adapted from Aiello and Dean (1990). **(B) Changes in the maximum circumference of the thorax during respiration due to pump-handle (dorsoventral; red) and bucket-handle (mediolateral; blue) motions in humans.** The shape of the thorax during inspiration is represented by dashed lines and expiration is represented by dotted lines.

(A)

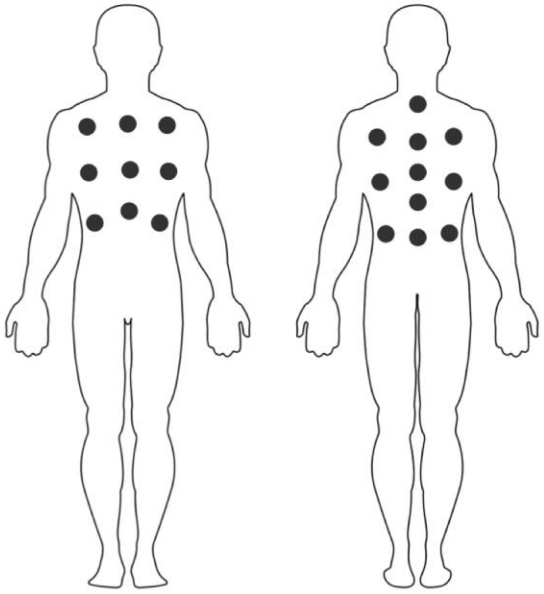

(B)

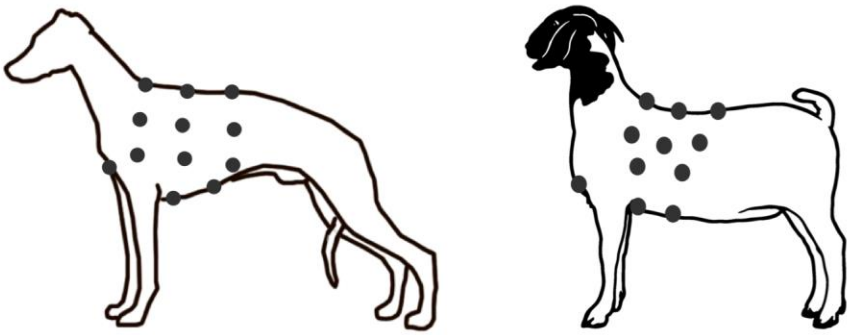

Figure 2: (A) Approximate reflective marker placement on human participants, ventral and dorsal views. (B) Approximate reflective marker placement on dog and goat subjects, sagittal view.

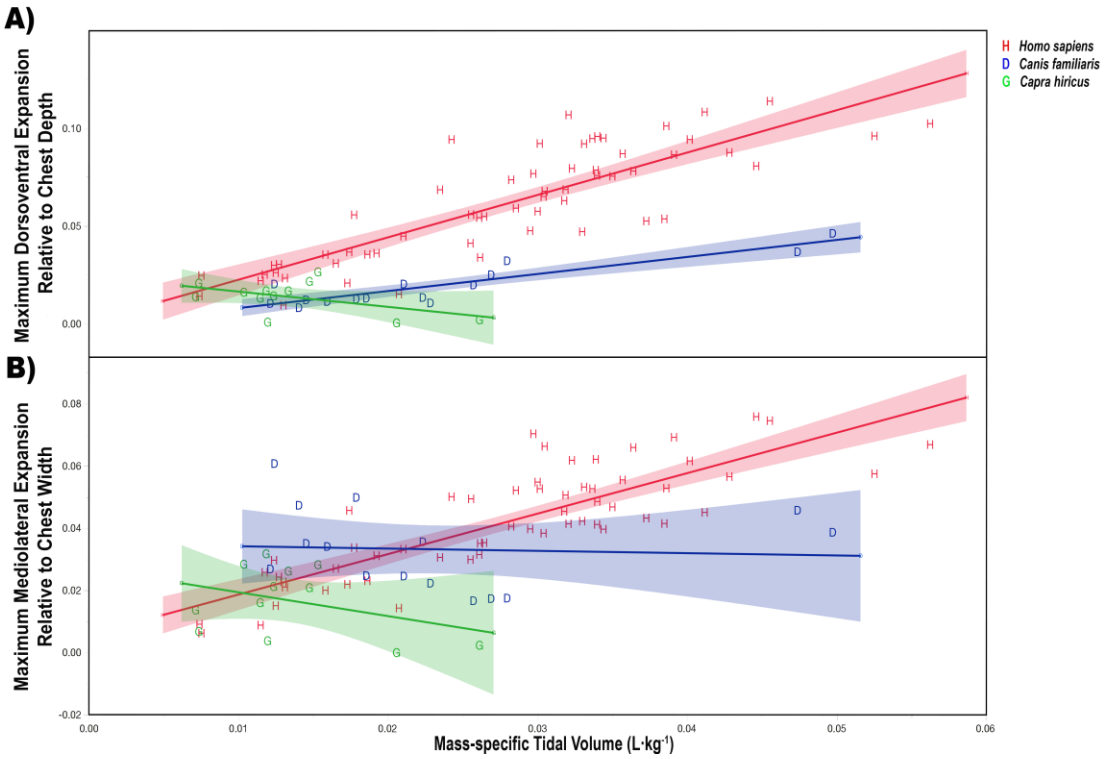

Figure 3: (A) Maximum dorsoventral thoracic expansion and (B) maximum mediolateral thoracic expansion relative to mass-specific tidal volume in humans, dogs and goats. (A) Maximum dorsoventral thoracic expansion increased with V_T [L•kg^{-1}] in humans and in dogs, but decreased in goats with increasing V_T [L•kg^{-1}]. (B) Maximum mediolateral thoracic expansion increased with V_T [L•kg^{-1}] in humans. Maximum mediolateral thoracic expansion decreased weakly in dogs and strongly in goats with increasing V_T [L•kg^{-1}]. Shading represent CI=0.95.

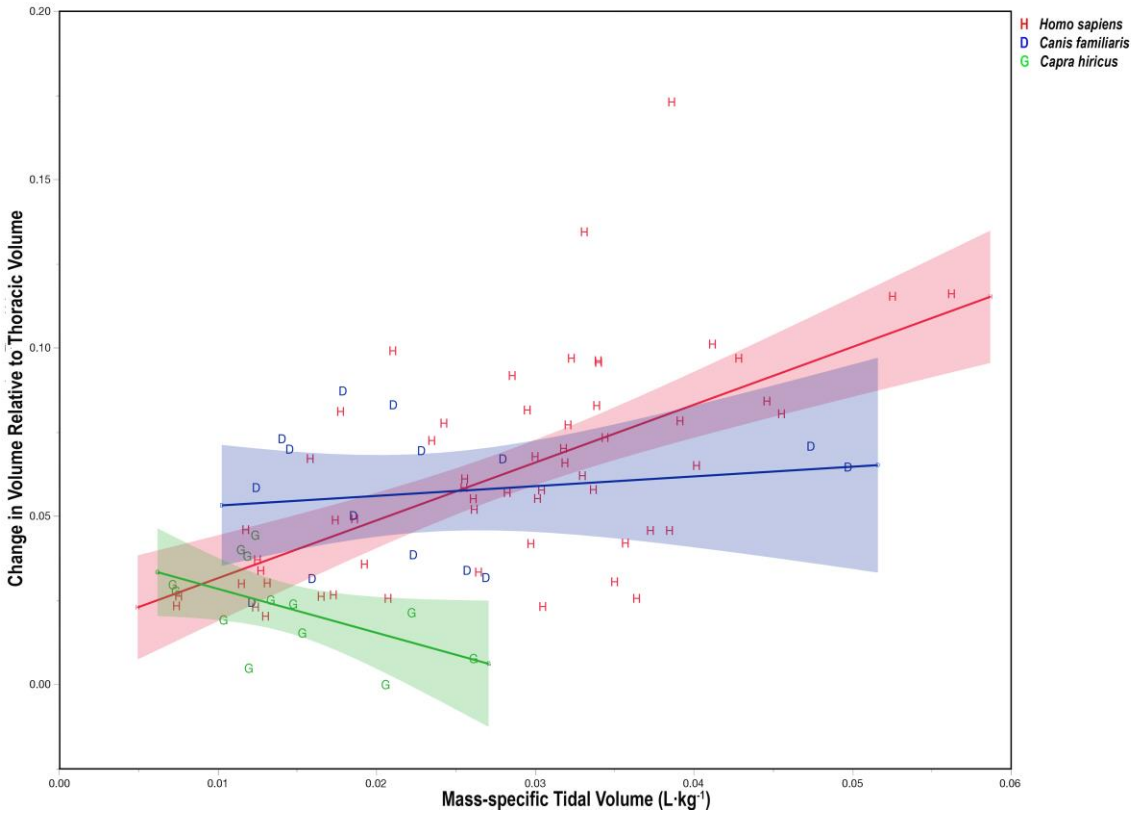

Figure 4: Change in thoracic volume during ventilation with change in mass-specific tidal volume in humans, dogs and goats. Change in thoracic volume during ventilation increased in humans and weakly in dogs (p=0.0146) as V_T [L•kg^{-1}] increased. Change in thoracic volume decreased in goats and was significantly different from humans (p<0.0001) and dogs (p=0.0445). Shading represent CI=0.95.

(A)

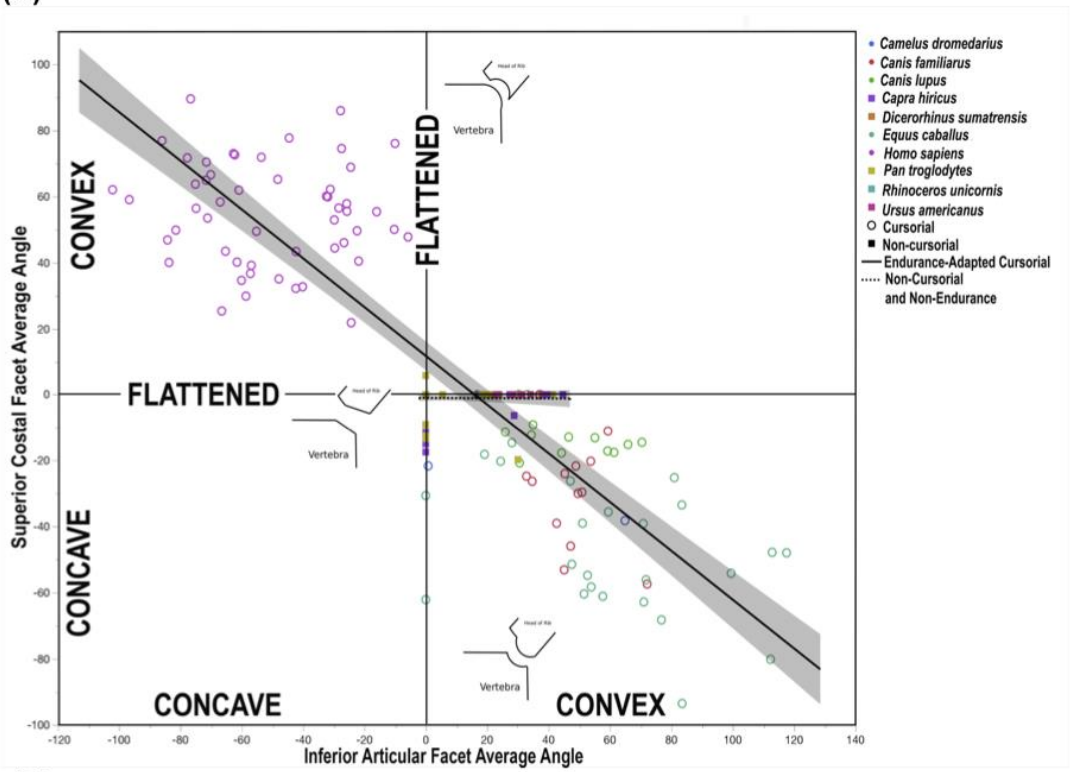

(B)

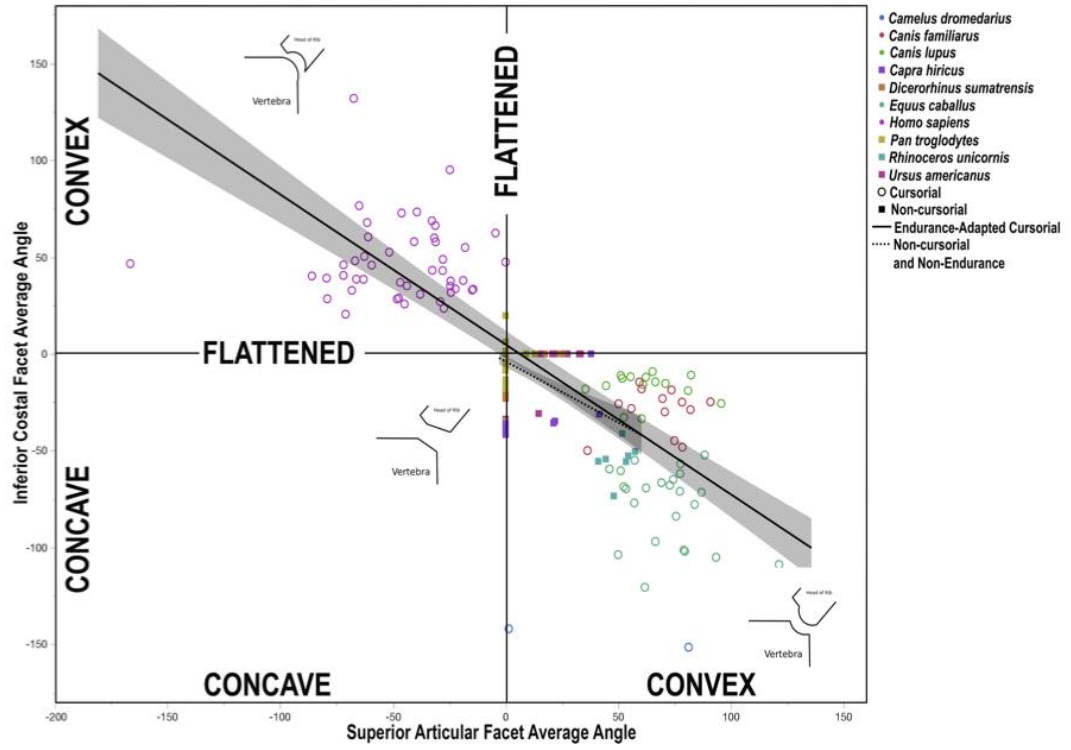

Figure 5: Relationships between rib and vertebral elements of the costovertebral joint in endurance-adapted cursorial species and non-endurance or non-cursorial species. Endurance-adapted cursorial species exhibit greater joint facet curvature than non-endurance and non-cursorial species within the same order (indicated by color) in the upper portion (A) and lower portion (B) of the costovertebral joint. Rib facet included angle corresponds strongly with vertebral facet included angle in endurance-adapted cursorial specimens, but not in non-endurance and non-cursorial specimens. Negative included angle values indicate concave joint facets, while positive values indicate convexity. Larger values are associated with greater joint concavo-convexity. Angle values of 0 indicate a flat facet.

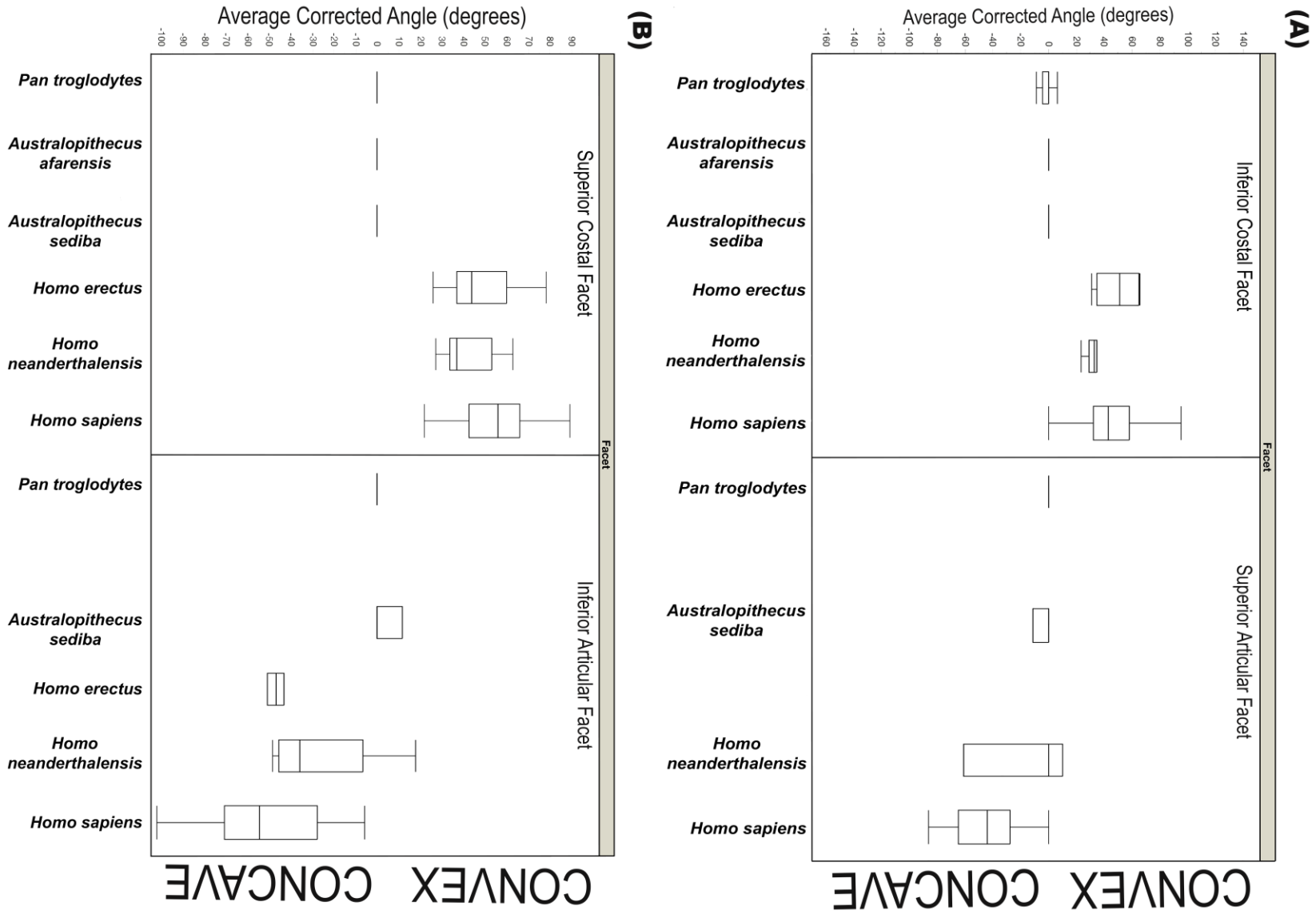
(A)
Average Corrected Angle (degrees)
-160 -140 -120 -100 -80 -60 -40 -20 0 20 40 60 80 100 120 140
Pan troglodytes
Australopithecus afarensis
Australopithecus sediba
Homo erectus
Homo neanderthalensis
Homo sapiens
Inferior Costal Facet
Superior Articular Facet
Facet
CONCAVE CONVEX
(B)
Average Corrected Angle (degrees)
-100 -90 -80 -70 -60 -50 -40 -30 -20 -10 0 10 20 30 40 50 60 70 80 90
Pan troglodytes
Australopithecus afarensis
Australopithecus sediba
Homo erectus
Homo neanderthalensis
Homo sapiens
Superior Costal Facet
Inferior Articular Facet
Facet
CONCAVE CONVEX

Figure 6: Differences in costovertebral joint morphology among hominid species in the superior (A) and inferior (B) sites of articulation in costovertebral joint. Australopiths exhibit a chimp-like joint morphology while *Homo* species are all similar in morphology. Negative included angle values indicate concave joint facets, while positive values indicate convexity. Larger values are associated with greater joint concavo-convexity. Angle values of 0 indicate a flat facet.

TABLES

Table 1: Differences in inferior costal facet (ICF), superior articular facet (SAF), superior costal facet (SCF) and inferior articular facet (IAF) curvature between species within the same order.

Comparison	Facet	Difference in Average Facet Included Angle (degrees)	Cohen's d	Effect Size (Cohen, 1988;, Sawilowsky, 2009)
Modern Human vs. Chimpanzee (*Primates*)	ICF	49.59 (SE=2.83; p<0.0001)*	0.98	Large
	SAF	46.70 (SE=3.71; p<0.0001)*	0.93	Large
	SCF	55.71 (SE=2.32; p<0.0001)*	1.11	Very Large
	IAF	54.22 (SE=3.75; p<0.0001)*	1.08	Very Large
Horse vs. Rhinoceros (*Perissodactyla*)	ICF	45.67 (SE=4.83; p<0.0001)*	0.91	Large
	SAF	41.92 (SE=6.12; p<0.0001)*	0.83	Large
	SCF	47.52 (SE=3.97; p<0.0001)*	0.94	Large
	IAF	56.89 (SE=6.49; p<0.0001)*	1.13	Very Large
Camel vs. Goat (*Artiodactyla*)	ICF	129.49 (SE=4.83; p<0.0001)*	2.57	Huge
	SAF	54.95 (SE=11.83; p=0.0001)*	1.09	Large
	SCF	9.43 (SE=3.97; p=0.8890)	0.19	Small
	IAF	21.60 (SE=14.58; p=0.9870)	0.43	Medium
Canine vs. Bear (*Carnivora*)	ICF	21.20 (SE=4.04; p<0.0001)*	0.42	Medium
	SAF	55.60 (SE=5.23; p<0.0001)*	1.11	Very Large
	SCF	19.73 (SE=3.32; p=0.0047)*	0.39	Medium
	IAF	33.51 (SE=5.43; p<0.0001)*	0.66	Medium

*Significant difference (p<0.05) between species of the same order.

Table 2: Measured costovertebral included angles across sampled hominids. Negative included angle values indicate concave joint facets, while positive values indicate convexity. Larger values are associated with greater joint concavo-convexity. Angle values of 0 indicate a flat facet.

Species	Number of Specimens	Mean Inferior Costal Facet (degrees)	Mean Superior Articular Facet (degrees)	Mean Superior Costal Facet (degrees)	Mean Inferior Articular Facet (degrees)
Pan troglodytes	8	-3.35 (SE=1.87, N=70)	0.410 (SE=2.55, N=54)	-1.04 (SE=1.58, N=56)	3.69 (SE=2.57, N=54)
Australopithecus afarensis **(AL-288)**	1	0.00 (SE=11.08, N=2)		0.00 (SE=8.35, N=2)	
Australopithecus sediba **(MH1 and MH2)**	2	0.67 (SE=0.67, N=14)	-3.82 (SE=10.84, N=3)	0.00 (SE=3.94, N=9)	3.95 (SE=10.90, N=3)
Homo erectus **(KNM-WT15000)**	1	48.26 (SE=5.92, N=7)		47.78 (SE=4.82, N=6)	-47.06 (SE=13.35, N=2)
Homo neanderthalensis **(Shanidar 2, Shanidar 3, Dederiyeh 2)**	3	32.94 (SE=5.54, N=8)	-17.11 (SE=10.84, N=3)	41.34 (SE=4.47, N=7)	-28.02 (SE=8.44, N=5)
Homo sapiens	9	46.24 (SE=1.87, N=70)	-46.29 (SE=2.7, N=47)	54.67 (SE=1.58, N=56)	-50.56 (SE=2.62, N=52)

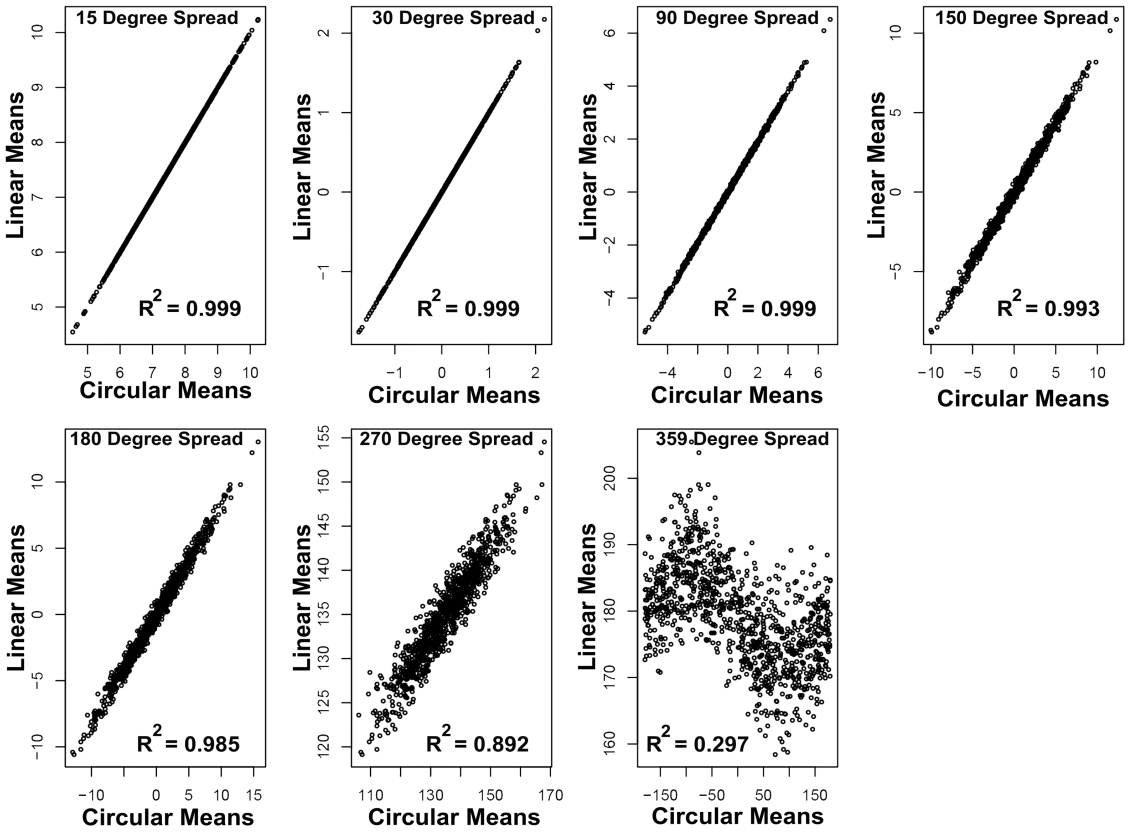

Figure S1: Circular means versus linear means from randomly generated angular data. Means calculated from 200 simulated angular data points across a desired angular spread were assessed in R (version 3.1.1) using linear and circular analyses. As spread of angular measurements increases, the ability to use linear analyses on circular data decreases (R^2 decreases). However, with a 150-degree spread (approximating our collected included angle data), circular data behaves linearly (R^2=0.9931), making linear analyses acceptable. Plots and analyses produced with the help of Steven Worthington at the Institute for Quantitative Social Science, Harvard University.

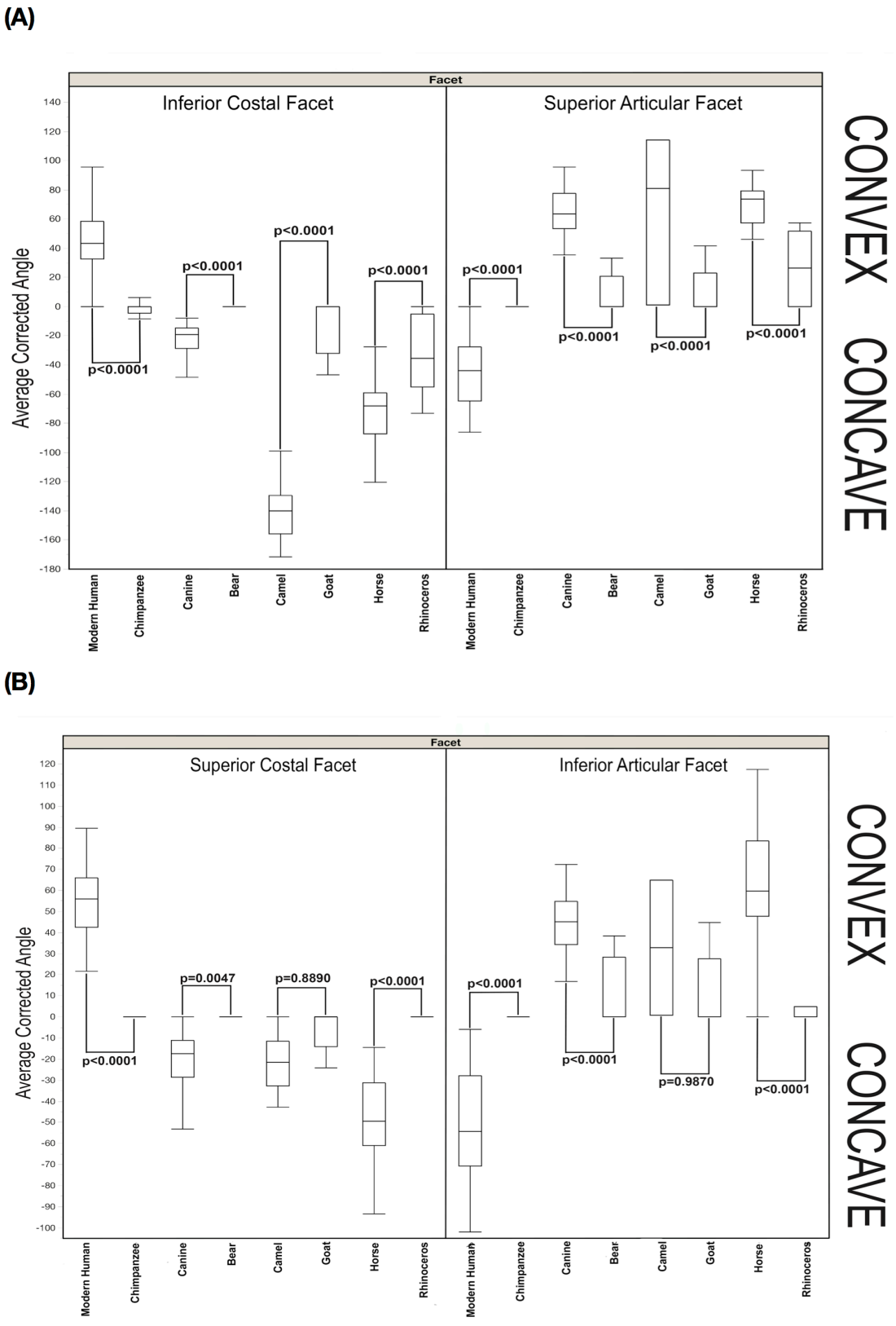

Figure S2: Differences in costovertebral joint morphology between closely related

endurance-adapted cursors and non-endurance extant species in the superior (A) and inferior (B) sites of articulation in costovertebral joint. Negative included angel values indicate convex joint facets, while positive values indicate concavity. Larger values are associated with greater joint curvature. Endurance-adapted cursorial species generally exhibited increased curvature relative to closely related non-cursorial species within the same Order.

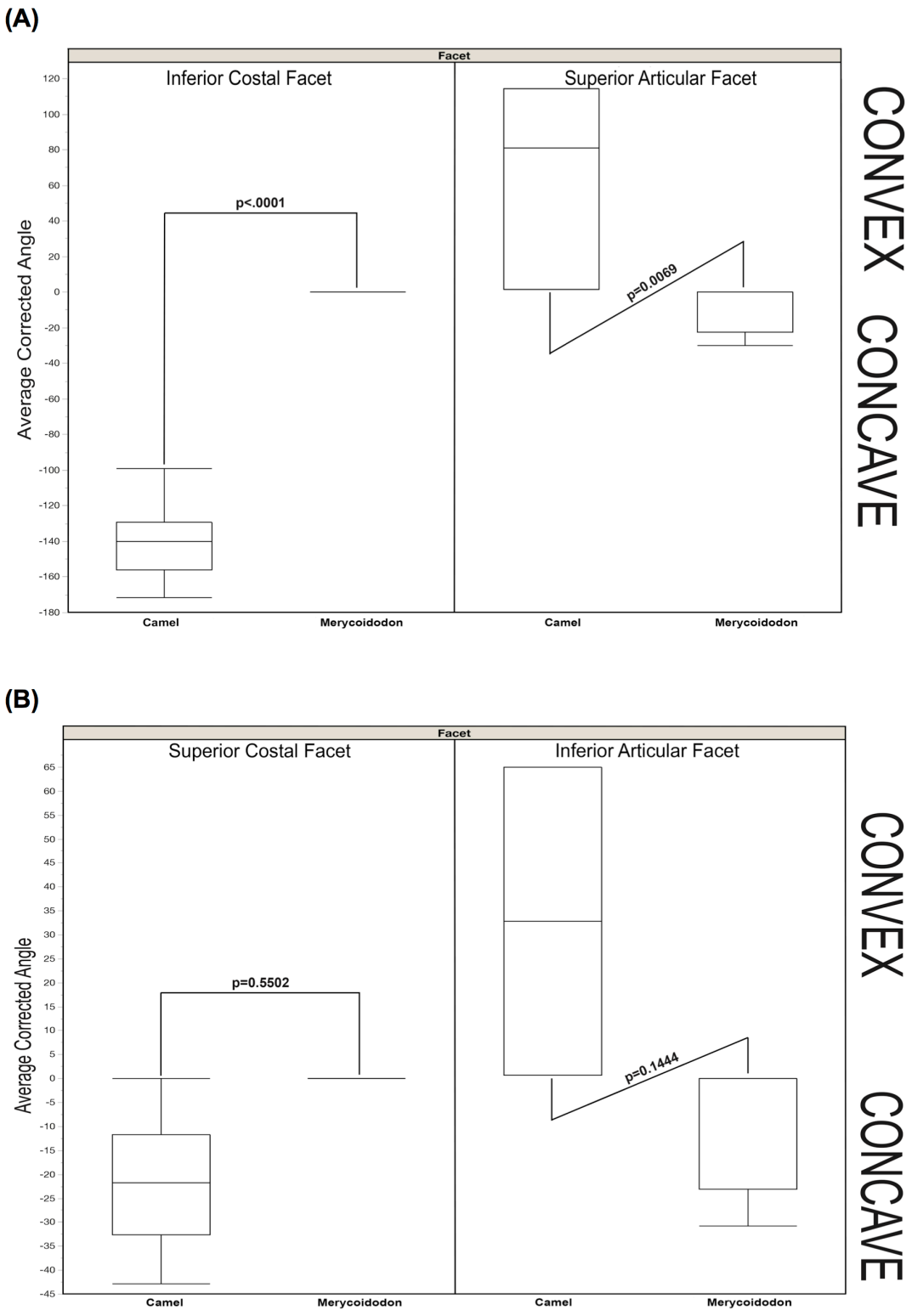

Figure S3: Differences in costovertebral joint morphology between extant camels and *Merycoidodon culbertsoni* in the superior (A) and inferior (B) sites of articulation in costovertebral joint. Negative included angel values indicate convex joint facets, while

positive values indicate concavity. Larger values are associated with greater joint curvature. Camels exhibited increased curvature in the upper site of articulation. As with camels and goats, camels differ from *Merycoidodon* at the superior site of articulation of the costovertebral joint. The superior site of articulation in camels exhibits an almost ball-and-socket joint-architecture and appears to be the primary articulation point between the vertebrae and heads of the ribs. The inferior site of articulation of the costovertebral joint appears reduced, with the superior site of articulation being primarily responsible for rib movement.

Table S1: Measurements of heart rate (HR), tidal volume (V_T) and respiration rate (f_R) in humans, dogs and goats. Estimated HR_{MAX} values are calculated based on $\dot{V}O_2$ and associated HR measurements (taken when the animals where trotting at the fastest speeds they would sustain) and previously measured $\dot{V}O_{2MAX}$ values for dogs (Lucas et al., 1980) and for goats (Taylor et al., 1980) ($HR_{MAX} = \frac{HR_{measured} \times VO_{2MAX}}{VO_{2measured}}$).

Participant/ Subject ID	Species	Body Mass (kg)	HR_{MAX} * indicates estimated value calculated from $\dot{V}O_2$. [R] indicates values reported elsewhere.	HR (beat/min)	V_T (L)	f_R (breaths/min)
R1	*Homo sapiens*	65.6	182	49	1.362	23
				76	1.223	22
				111	2.087	29
				140	2.811	33
				179	3.691	37
				182	3.447	37
R2	*Homo sapiens*	69.6	191	60	0.872	13
				97	0.914	31
				135	2.09	32
				153	2.36	35
				183	2.689	44
				191	2.397	50
R3	*Homo sapiens*	72.7	188	66	1.152	21
				87	1.291	24
				120	2.472	34
				154	2.473	45
				178	2.449	56
				178	2.055	51
R4	*Homo sapiens*	65.3	196	73	0.851	9
				86	1.13	21
				125	1.71	30
				153	2.155	33
				191	2.435	45
				193	2.514	49
S1	*Homo sapiens*	66.7	194	72	1.969	16
				96	1.906	19
				141	2.156	30
				154	2.21	37
				190	2.013	62
				196	1.619	42

S2	*Homo sapiens*	77.1	188	64	0.909	12
				92	1.276	25
				113	1.624	47
				155	2.46	48
				185	2.754	53
S3	*Homo sapiens*	56.3	200	69	0.426	30
				86	0.717	24
				119	1.323	29
				195	2.32	39
				196	1.807	47
S4	*Homo sapiens*	70.9	186	69	1.236	12
				75	1.366	19
				115	1.814	24
				152	3.165	31
				180	2.582	61
				178	2.109	49
S5	*Homo sapiens*	84.8	196	58	0.976	14
				94	2.166	17
				120	2.215	44
				152	2.58	36
				188	2.971	57
				186	2.243	62
S6	*Homo sapiens*	78.6	184	61	0.583	23
				80	0.975	32
				113	2.398	30
				151	3.077	35
				178	3.58	46
				177	3.16	47
G1	*Capra hiricus*	40	258*	139	0.824	89
			209 ± 8^{R} (Hohimer et al., 1984)	191	0.614	122
				205	0.591	147
				218	0.295	186
				230	0.287	189
G2	*Capra hiricus*	27.69	236	131	0.724	69
			209 ± 8^{R} (Hohimer et al., 1984)	180	0.343	77
				218	0.318	89
				236	0.616	97
G3	*Capra hiricus*	41.9	239*	111	0.502	63
			209 ± 8^{R} (Hohimer et al., 1984)	169	0.498	72

				183	0.56	81
				222	0.435	108
D1	*Canis familiaris*	35.7	313*	93	1.776	23
			294±5^{R} (Lucas et al., 1980)	145	0.816	32
				155	0.663	36
				151	0.57	32
				147	0.434	77
D2	*Canis familiaris*	31.06	314*	62	1.472	23
			294±5^{R} (Lucas et al., 1980)	116	0.556	38
				109	0.452	29
				109	0.437	29
				105	0.386	44
D3	*Canis familiaris*	25.96	312*	56	0.58	24
			294±5^{R} (Lucas et al., 1980)	84	0.668	22
				96	0.699	22
				93	0.727	23
				93	0.547	24

Table S2: Repeatability of included angle measurements for the inferior costal facet (ICF), superior articular facet (SAF), superior costal facet (SCF) and inferior articular facet (IAF).

Species	**Facet**	**% of Total Variation due to Repeated Measurement**	**Repeatability** (Barrentine, 1991)
Homo sapiens	SAF	<1	Excellent
	IAF	<1	Excellent
	SCF	<1	Excellent
	ICF	<1	Excellent
Pan troglodytes	SAF	<1	Excellent
	IAF	<1	Excellent
	SCF	<1	Excellent
	ICF	<1	Excellent
Equus caballus	SAF	<1	Excellent
	IAF	<1	Excellent
	SCF	<1	Excellent
	ICF	<1	Excellent
Rhinoceros unicornis **and** ***Dicerorhinus sumatrensis***	SAF	<1	Excellent
	IAF	<1	Excellent
	SCF	<1	Excellent
	ICF	<1	Excellent
Canus familiaris **and** ***Canus lupus***	SAF	<1	Excellent
	IAF	<1	Excellent
	SCF	<1	Excellent
	ICF	<1	Excellent
Ursus americanus	SAF	<1	Excellent
	IAF	<1	Excellent
	SCF	<1	Excellent
	ICF	<1	Excellent
Camelus dromedarius	SAF	<1	Excellent
	IAF	<1	Excellent
	SCF	<1	Excellent
	ICF	<1	Excellent
Capra hiricus	SAF	<1	Excellent
	IAF	<1	Excellent
	SCF	<1	Excellent
	ICF	<1	Excellent
H. neanderthalensis	SAF	<1	Excellent
	IAF	<1	Excellent
	SCF	<1	Excellent
	ICF	<1	Excellent
H. erectus	SAF		
	IAF	<1	Excellent
	SCF	<1	Excellent
	ICF	<1	Excellent
Au. sediba	SAF	<1	Excellent
	IAF	<1	Excellent
	SCF	<1	Excellent
	ICF	<1	Excellent

Au. afarensis	SAF		
	IAF		
	SCF	<1	Excellent
	ICF	<1	Excellent
Merycoidodon culbertsoni	SAF	<1	Excellent
	IAF	<1	Excellent
	SCF	<1	Excellent
	ICF	<1	Excellent

Table S3: Measured inferior costal facet (ICF), superior articular facet (SAF), superior costal facet (SCF) and inferior articular facet (IAF) included angles across sampled species. Negative included angle values indicate concave joint facets, while positive values indicate convexity. Larger values are associated with greater joint concavo-convexity. Angle values of 0 indicate a flat facet.

Species	Facet	Number of samples	Mean Angle (degrees)	Std. Error
Homo sapiens	SAF	47	-46.29	2.75
	IAF	52	-50.56	2.62
	SCF	56	54.67	1.58
	ICF	70	46.24	1.87
Pan troglodytes	SAF	54	0.41	2.55
	IAF	54	3.69	13.35
	SCF	56	-1.04	4.82
	ICF	70	-3.35	1.87
Equus caballus	SAF	24	71.36	3.83
	IAF	24	61.40	3.94
	SCF	24	-47.52	2.41
	ICF	30	-73.03	2.86
Rhinoceros unicornis and ***Dicerorhinus sumatrensis***	SAF	15	29.44	4.85
	IAF	14	4.51	5.04
	SCF	16	0.00	2.95
	ICF	20	-27.37	3.92
Canus familiaris and ***Canus lupus***	SAF	28	64.79	3.55
	IAF	28	45.20	3.57
	SCF	32	-19.73	2.09
	ICF	40	-23.35	2.48
Ursus americanus	SAF	23	9.19	3.91
	IAF	23	11.70	3.94
	SCF	24	0.00	2.41

	ICF	30	-2.15	2.86
Camelus dromedarius	SAF	3	65.56	10.84
	IAF	2	32.84	13.35
	SCF	16	-15.95	3.41
	ICF	20	-140.29	3.50
Capra hiricus	SAF	14	10.61	5.02
	IAF	14	11.24	5.04
	SCF	24	-6.53	2.41
	ICF	30	-10.80	2.86
H. neanderthalensis	SAF	3	-17.11	10.84
	IAF	5	-28.02	8.44
	SCF	7	41.34	4.47
	ICF	8	32.94	5.54
H. erectus	SAF			
	IAF	2	-47.06	13.35
	SCF	6	47.78	4.82
	ICF	7	48.26	5.92
Au. sediba	SAF	3	-3.82	10.84
	IAF	3	3.95	10.90
	SCF	9	0.00	3.94
	ICF	14	0.67	4.19
Au. afarensis	SAF			
	IAF			
	SCF	2	0.00	8.35
	ICF	2	0.00	11.08
Merycoidodon culbertsoni	SAF	4	-7.47	9.38
	IAF	4	-7.67	9.44

	SCF	13	2.06	3.28
	ICF	14	0.00	4.19

References:

Barrentine, L.B. (1991). *Concepts for R&R Studies*. Milwaukee, WI: ASQ Quality Press.

Hohimer, A.R., Bissonnette, J.M., Metcalfe, J., McKean, T.A. (1984). Effect of exercise on uterine blood flow in the pregnant Pygmy goat. *American Journal of Physiology*, **246**(2 Pt 2), H207-12.

Lucas A., Therminarias, A., Tanche, M. (1980). Maximum oxygen consumption in dogs during muscular exercise and cold exposure. *Pflügers Archiv European Journal of Physiology* **388**, 83-87.

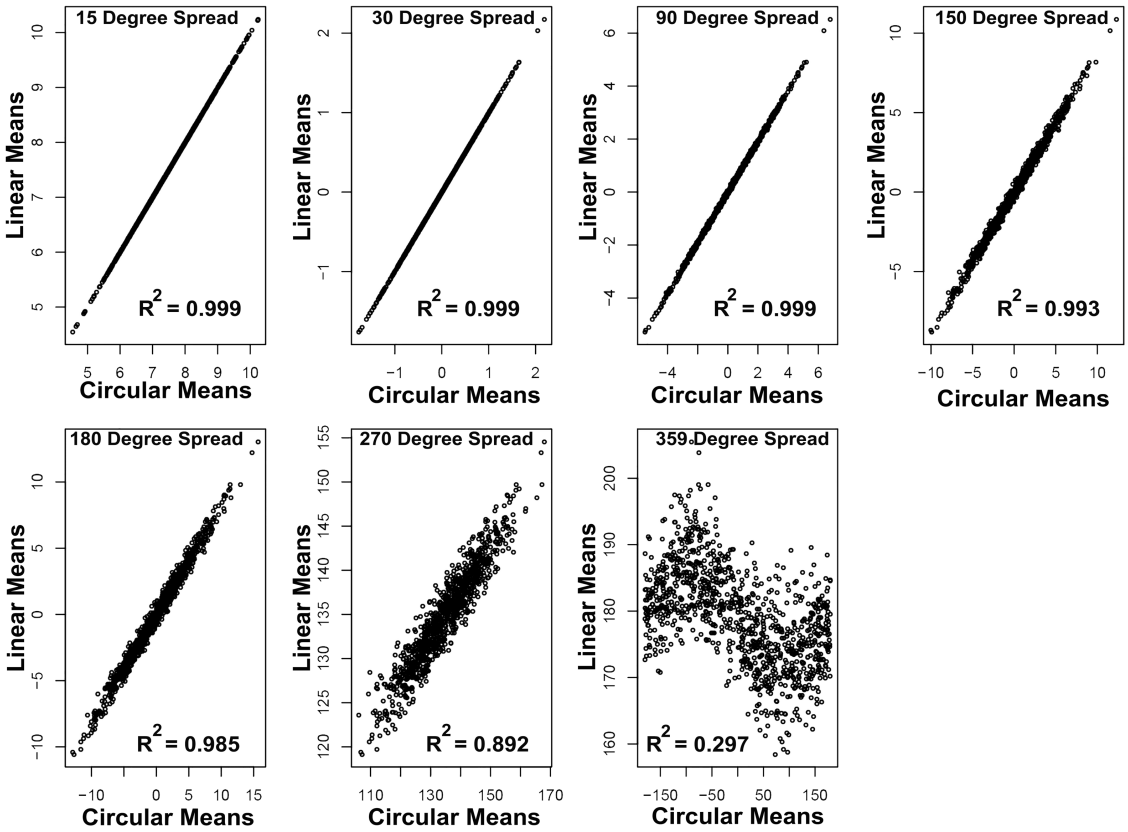

Figure S1: Circular means versus linear means from randomly generated angular data. Means calculated from 200 simulated angular data points across a desired angular spread were assessed in R (version 3.1.1) using linear and circular analyses. As spread of angular measurements increases, the ability to use linear analyses on circular data decreases (R^2 decreases). However, with a 150-degree spread (approximating our collected included angle data), circular data behaves linearly (R^2=0.9931), making linear analyses acceptable. Plots and analyses produced with the help of Steven Worthington at the Institute for Quantitative Social Science, Harvard University.

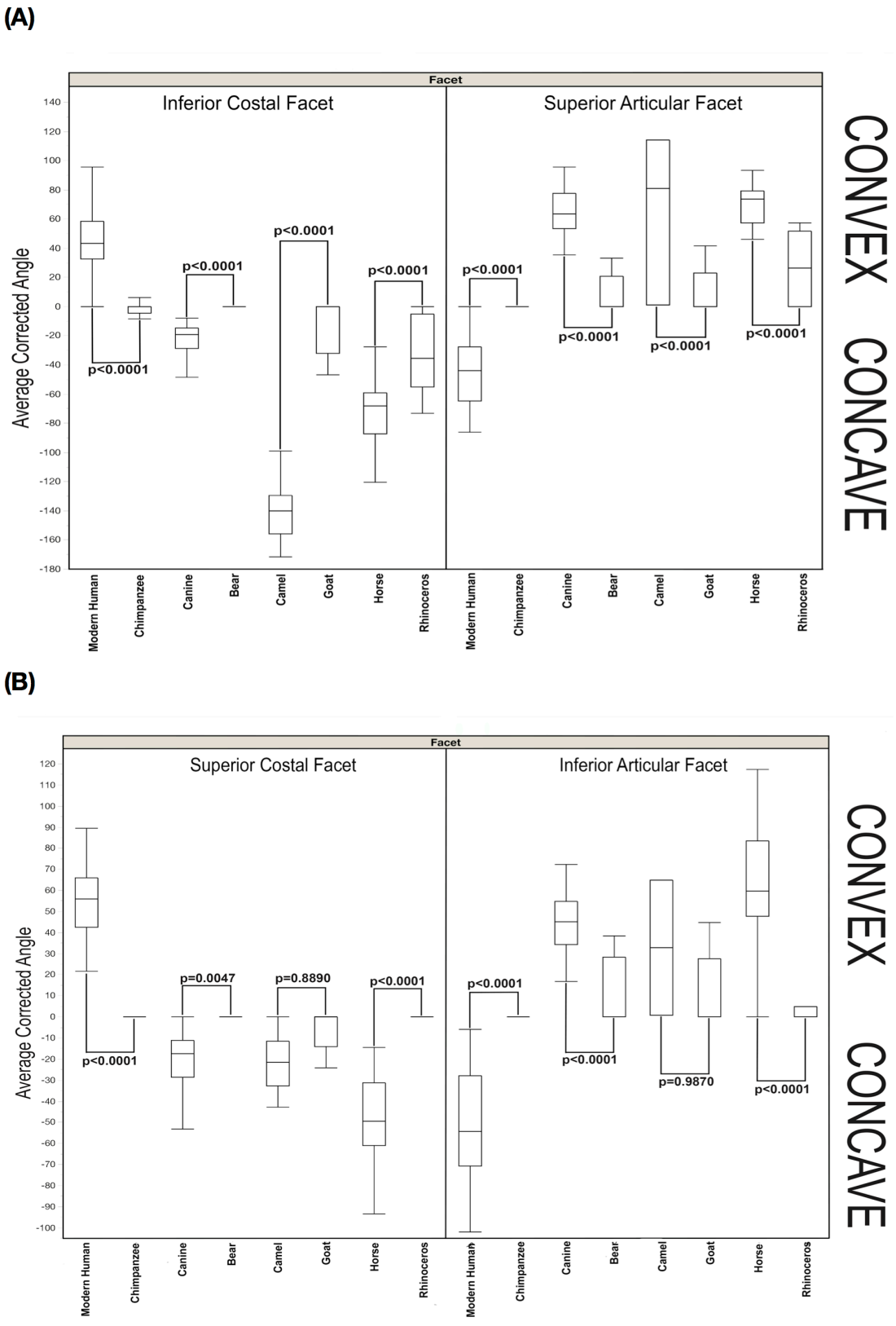

Figure S2: Differences in costovertebral joint morphology between closely related

endurance-adapted cursors and non-endurance extant species in the superior (A) and inferior (B) sites of articulation in costovertebral joint. Negative included angel values indicate convex joint facets, while positive values indicate concavity. Larger values are associated with greater joint curvature. Endurance-adapted cursorial species generally exhibited increased curvature relative to closely related non-cursorial species within the same Order.

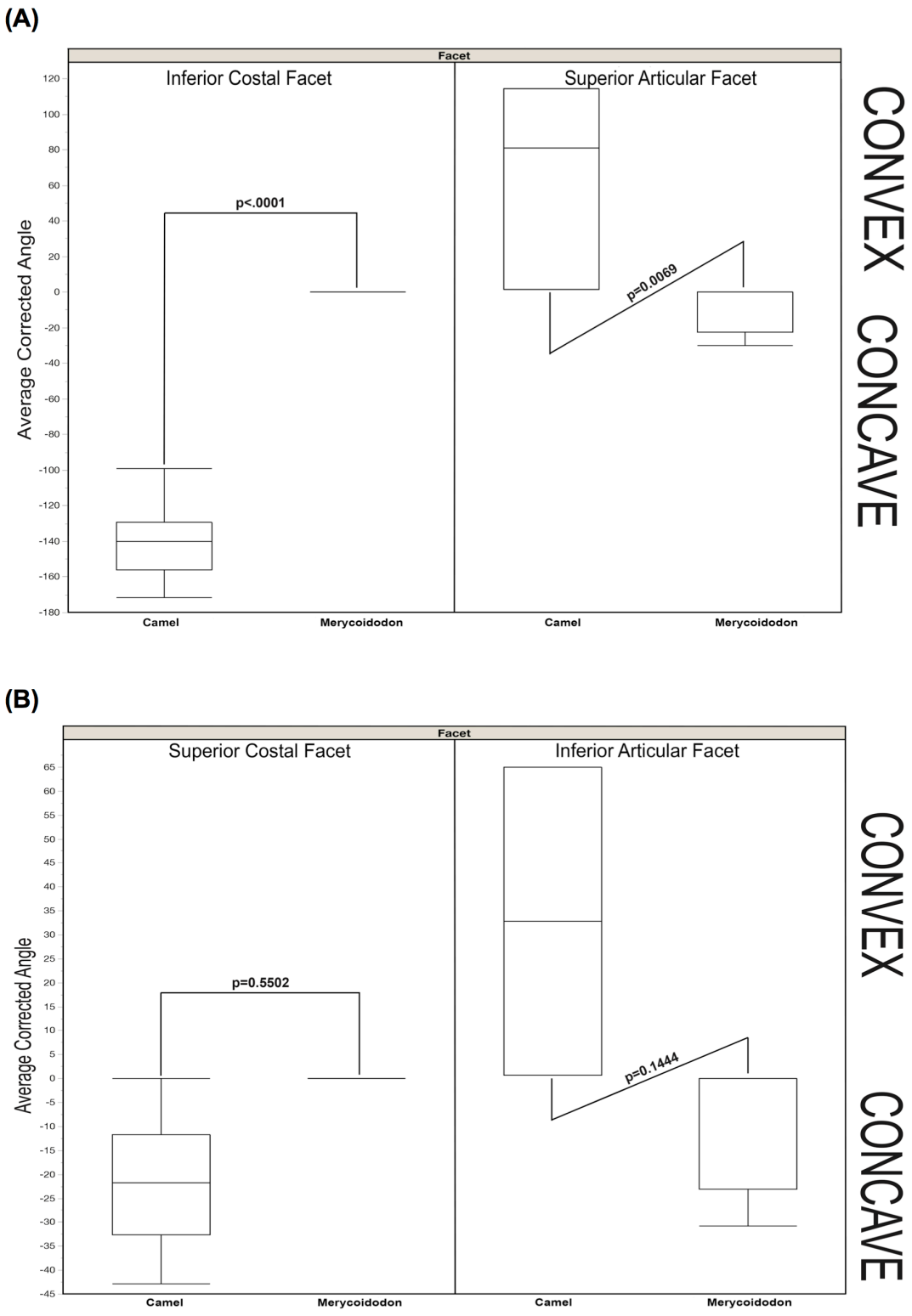

Figure S3: Differences in costovertebral joint morphology between extant camels and *Merycoidodon culbertsoni* in the superior (A) and inferior (B) sites of articulation in costovertebral joint. Negative included angel values indicate convex joint facets, while

positive values indicate concavity. Larger values are associated with greater joint curvature. Camels exhibited increased curvature in the upper site of articulation. As with camels and goats, camels differ from *Merycoidodon* at the superior site of articulation of the costovertebral joint. The superior site of articulation in camels exhibits an almost ball-and-socket joint-architecture and appears to be the primary articulation point between the vertebrae and heads of the ribs. The inferior site of articulation of the costovertebral joint appears reduced, with the superior site of articulation being primarily responsible for rib movement.

Table S1: Measurements of heart rate (HR), tidal volume (V_T) and respiration rate (f_R) in humans, dogs and goats. Estimated HR_{MAX} values are calculated based on $\dot{V}O_2$ and associated HR measurements (taken when the animals where trotting at the fastest speeds they would sustain) and previously measured $\dot{V}O_{2MAX}$ values for dogs (Lucas et al., 1980) and for goats (Taylor et al., 1980) ($HR_{MAX} = \frac{HR_{measured} \times VO_{2MAX}}{VO_{2measured}}$).

Participant/ Subject ID	Species	Body Mass (kg)	HR_{MAX} * indicates estimated value calculated from $\dot{V}O_2$. [R] indicates values reported elsewhere.	HR (beat/min)	V_T (L)	f_R (breaths/min)
R1	*Homo sapiens*	65.6	182	49	1.362	23
				76	1.223	22
				111	2.087	29
				140	2.811	33
				179	3.691	37
				182	3.447	37
R2	*Homo sapiens*	69.6	191	60	0.872	13
				97	0.914	31
				135	2.09	32
				153	2.36	35
				183	2.689	44
				191	2.397	50
R3	*Homo sapiens*	72.7	188	66	1.152	21
				87	1.291	24
				120	2.472	34
				154	2.473	45
				178	2.449	56
				178	2.055	51
R4	*Homo sapiens*	65.3	196	73	0.851	9
				86	1.13	21
				125	1.71	30
				153	2.155	33
				191	2.435	45
				193	2.514	49
S1	*Homo sapiens*	66.7	194	72	1.969	16
				96	1.906	19
				141	2.156	30
				154	2.21	37
				190	2.013	62
				196	1.619	42

S2	*Homo sapiens*	77.1	188	64	0.909	12
				92	1.276	25
				113	1.624	47
				155	2.46	48
				185	2.754	53
S3	*Homo sapiens*	56.3	200	69	0.426	30
				86	0.717	24
				119	1.323	29
				195	2.32	39
				196	1.807	47
S4	*Homo sapiens*	70.9	186	69	1.236	12
				75	1.366	19
				115	1.814	24
				152	3.165	31
				180	2.582	61
				178	2.109	49
S5	*Homo sapiens*	84.8	196	58	0.976	14
				94	2.166	17
				120	2.215	44
				152	2.58	36
				188	2.971	57
				186	2.243	62
S6	*Homo sapiens*	78.6	184	61	0.583	23
				80	0.975	32
				113	2.398	30
				151	3.077	35
				178	3.58	46
				177	3.16	47
G1	*Capra hiricus*	40	258*	139	0.824	89
			209 ± 8^{R} (Hohimer et al., 1984)	191	0.614	122
				205	0.591	147
				218	0.295	186
				230	0.287	189
G2	*Capra hiricus*	27.69	236	131	0.724	69
			209 ± 8^{R} (Hohimer et al., 1984)	180	0.343	77
				218	0.318	89
				236	0.616	97
G3	*Capra hiricus*	41.9	239*	111	0.502	63
			209 ± 8^{R} (Hohimer et al., 1984)	169	0.498	72

				183	0.56	81
				222	0.435	108
D1	*Canis familiaris*	35.7	313*	93	1.776	23
			294±5^{R} (Lucas et al., 1980)	145	0.816	32
				155	0.663	36
				151	0.57	32
				147	0.434	77
D2	*Canis familiaris*	31.06	314*	62	1.472	23
			294±5^{R} (Lucas et al., 1980)	116	0.556	38
				109	0.452	29
				109	0.437	29
				105	0.386	44
D3	*Canis familiaris*	25.96	312*	56	0.58	24
			294±5^{R} (Lucas et al., 1980)	84	0.668	22
				96	0.699	22
				93	0.727	23
				93	0.547	24

Table S2: Repeatability of included angle measurements for the inferior costal facet (ICF), superior articular facet (SAF), superior costal facet (SCF) and inferior articular facet (IAF).

Species	**Facet**	**% of Total Variation due to Repeated Measurement**	**Repeatability** (Barrentine, 1991)
Homo sapiens	SAF	<1	Excellent
	IAF	<1	Excellent
	SCF	<1	Excellent
	ICF	<1	Excellent
Pan troglodytes	SAF	<1	Excellent
	IAF	<1	Excellent
	SCF	<1	Excellent
	ICF	<1	Excellent
Equus caballus	SAF	<1	Excellent
	IAF	<1	Excellent
	SCF	<1	Excellent
	ICF	<1	Excellent
Rhinoceros unicornis **and** ***Dicerorhinus sumatrensis***	SAF	<1	Excellent
	IAF	<1	Excellent
	SCF	<1	Excellent
	ICF	<1	Excellent
Canus familiaris **and** ***Canus lupus***	SAF	<1	Excellent
	IAF	<1	Excellent
	SCF	<1	Excellent
	ICF	<1	Excellent
Ursus americanus	SAF	<1	Excellent
	IAF	<1	Excellent
	SCF	<1	Excellent
	ICF	<1	Excellent
Camelus dromedarius	SAF	<1	Excellent
	IAF	<1	Excellent
	SCF	<1	Excellent
	ICF	<1	Excellent
Capra hiricus	SAF	<1	Excellent
	IAF	<1	Excellent
	SCF	<1	Excellent
	ICF	<1	Excellent
H. neanderthalensis	SAF	<1	Excellent
	IAF	<1	Excellent
	SCF	<1	Excellent
	ICF	<1	Excellent
H. erectus	SAF		
	IAF	<1	Excellent
	SCF	<1	Excellent
	ICF	<1	Excellent
Au. sediba	SAF	<1	Excellent
	IAF	<1	Excellent
	SCF	<1	Excellent
	ICF	<1	Excellent

Au. afarensis	SAF		
	IAF		
	SCF	<1	Excellent
	ICF	<1	Excellent
Merycoidodon culbertsoni	SAF	<1	Excellent
	IAF	<1	Excellent
	SCF	<1	Excellent
	ICF	<1	Excellent

Table S3: Measured inferior costal facet (ICF), superior articular facet (SAF), superior costal facet (SCF) and inferior articular facet (IAF) included angles across sampled species. Negative included angle values indicate concave joint facets, while positive values indicate convexity. Larger values are associated with greater joint concavo-convexity. Angle values of 0 indicate a flat facet.

Species	Facet	Number of samples	Mean Angle (degrees)	Std. Error
Homo sapiens	SAF	47	-46.29	2.75
	IAF	52	-50.56	2.62
	SCF	56	54.67	1.58
	ICF	70	46.24	1.87
Pan troglodytes	SAF	54	0.41	2.55
	IAF	54	3.69	13.35
	SCF	56	-1.04	4.82
	ICF	70	-3.35	1.87
Equus caballus	SAF	24	71.36	3.83
	IAF	24	61.40	3.94
	SCF	24	-47.52	2.41
	ICF	30	-73.03	2.86
Rhinoceros unicornis and ***Dicerorhinus sumatrensis***	SAF	15	29.44	4.85
	IAF	14	4.51	5.04
	SCF	16	0.00	2.95
	ICF	20	-27.37	3.92
Canus familiaris and ***Canus lupus***	SAF	28	64.79	3.55
	IAF	28	45.20	3.57
	SCF	32	-19.73	2.09
	ICF	40	-23.35	2.48
Ursus americanus	SAF	23	9.19	3.91
	IAF	23	11.70	3.94
	SCF	24	0.00	2.41

	ICF	30	-2.15	2.86
Camelus dromedarius	SAF	3	65.56	10.84
	IAF	2	32.84	13.35
	SCF	16	-15.95	3.41
	ICF	20	-140.29	3.50
Capra hiricus	SAF	14	10.61	5.02
	IAF	14	11.24	5.04
	SCF	24	-6.53	2.41
	ICF	30	-10.80	2.86
H. neanderthalensis	SAF	3	-17.11	10.84
	IAF	5	-28.02	8.44
	SCF	7	41.34	4.47
	ICF	8	32.94	5.54
H. erectus	SAF			
	IAF	2	-47.06	13.35
	SCF	6	47.78	4.82
	ICF	7	48.26	5.92
Au. sediba	SAF	3	-3.82	10.84
	IAF	3	3.95	10.90
	SCF	9	0.00	3.94
	ICF	14	0.67	4.19
Au. afarensis	SAF			
	IAF			
	SCF	2	0.00	8.35
	ICF	2	0.00	11.08
Merycoidodon culbertsoni	SAF	4	-7.47	9.38
	IAF	4	-7.67	9.44

	SCF	13	2.06	3.28
	ICF	14	0.00	4.19

References:

Barrentine, L.B. (1991). *Concepts for R&R Studies*. Milwaukee, WI: ASQ Quality Press.

Hohimer, A.R., Bissonnette, J.M., Metcalfe, J., McKean, T.A. (1984). Effect of exercise on uterine blood flow in the pregnant Pygmy goat. *American Journal of Physiology*, **246**(2 Pt 2), H207-12.

Lucas A., Therminarias, A., Tanche, M. (1980). Maximum oxygen consumption in dogs during muscular exercise and cold exposure. *Pflügers Archiv European Journal of Physiology* **388**, 83-87.